

pp 941–974. © Royal Aeronautical Society 2020  
doi:10.1017/aer.2019.164

# Review on ducted fans for compound rotorcraft

T. Zhang and G.N. Barakos<sup>id</sup>  
[george.barakos@glasgow.ac.uk](mailto:george.barakos@glasgow.ac.uk)

CFD Laboratory, School of Engineering  
University of Glasgow  
Glasgow  
UK

## ABSTRACT

This paper presents a survey of published works on ducted fans for aeronautical applications. Early and recent experiments on full- or model-scale ducted fans are reviewed. Theoretical studies, lower-order simulations and high-fidelity CFD simulations are also summarised. Test matrices of several experimental and numerical studies are compiled and discussed. The paper closes with a summary of challenges for future ducted fan research.

**Keywords:** Ducted rotor; Ducted fan; Propulsor

## NOMENCLATURE

$A$	propeller disk area
$A_e$	duct exit area
$AoA$	duct angle-of-attack
$c_{duct}$	duct profile chord length
$D_{in}$	duct inner diameter
$FoM$	figure of Merit
$Ma$	mach number
$P_{df}$	ducted fan power
$P_{op}$	open propeller power
$Re$	Reynolds number ( $Re = V_{\infty}c_{duct}/\nu_{\infty}$ )
$RPM$	revolutions per minute
$T_{df}$	duct fan thrust
$T_{op}$	open propeller thrust
$V_{\infty}$	free-stream speed
$V_{tip}$	blade tip speed
$\beta$	blade pitch angle at 70% radial section

$\Lambda$	expansion ratio, $\Lambda = A_e/A$
$\mu$	propeller advance ratio ( $\mu = V_\infty/nD$ )
$\nu_\infty$	free-stream kinematic viscosity
$\rho_\infty$	free-stream density
CFD	computational fluid dynamics
DDES	delayed detached Eddy simulation
eVTOL	electric vertical take-off and landing
MAV	micro aerial vehicle
PAV	personal aerial vehicle
PIV	particle image velocimetry
UAV	unmanned aerial vehicle
URANS	unsteady Reynolds averaged Navier–Stokes

## 1 INTRODUCTION

The ducted fan, or ducted/shrouded propeller concept, was first examined experimentally by Stipa<sup>(1)</sup> in the 1930s, and soon after it was widely studied using theory and further experiments. An overview of most early studies, before 1962, was presented by Sacks and Burnell.<sup>(2)</sup> Reviews on more recent studies can be found in the dissertations of Pereira,<sup>(3)</sup> and of Akturk and Camci,<sup>(4)</sup> although emphasis was put on UAV (Unmanned Aerial Vehicle) applications. A clear resurgence in ducted fan research in recent years can be noticed, due to the growing interest in UAV/MAV (Micro Aerial Vehicle), PAV (Personal Aerial Vehicle), and electric propulsion.

The ducted fan is a propeller inside a circular duct. It can be considered as a hybrid of a propeller and a turbofan engine, while the turbofan can be seen as a ducted fan driven by a turbojet. The duct is usually considered as an annular wing.<sup>(5)</sup> The duct brings superior static performance over its free propeller counterpart given the same power, as confirmed by many early-age experiments.<sup>(6–8)</sup> The performance gains are mainly attributed to the combined effect of suction on the curved duct inlet lip and the larger static pressure around the diffuser outlet.

A simple analysis for ideal hover cases can be made using momentum theory. For the same thrust required, the power reduction  $P_{df}/P_{op}$  can be written as a function of the expansion ratio  $\Lambda$ :

$$\frac{P_{df}}{P_{op}} = \frac{1}{\sqrt{2\Lambda}}, \quad \dots (1)$$

where  $df$  stands for ducted fan and  $op$  for open propeller.

Given the same power, the thrust improvement  $T_{df}/T_{op}$  can also be defined as a function of the expansion ratio  $\Lambda$ :

$$\frac{T_{df}}{T_{op}} = \sqrt[3]{2\Lambda}. \quad \dots (2)$$

It can thus be seen that performance improvements can be achieved, as long as  $\Lambda$  is kept greater than 0.5. The higher the expansion ratio  $\Lambda$ , the higher the performance improvement.

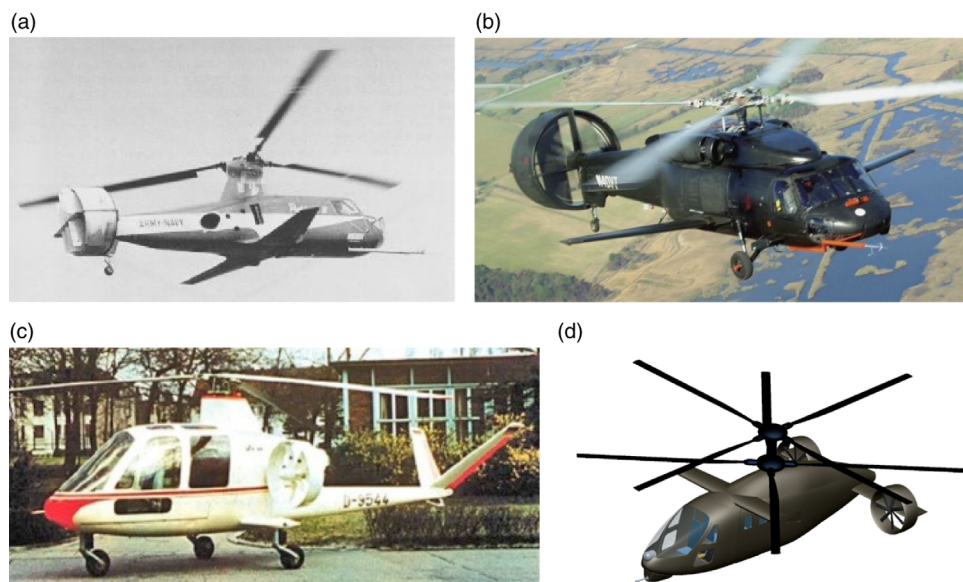


Figure 1. Ducted fan compound helicopter applications. (a) Piasecki 16H-1A. (b) Piasecki X-49A SpeedHawk. (c) VFW H3 Sprinter. (d) Coaxial Compound Helicopter (CCH) by Johnson et al.<sup>(13)</sup>

More detailed analyses using momentum theory can be found in Ref. [3]. In reality, the expansion ratio  $\Lambda$  is restricted by the adverse pressure gradient, which may lead to flow separation inside the diffuser.

Apart from UAV applications, the ducted fan can be an ideal choice for novel rotorcraft configurations. For instance, when installed on a compound helicopter, as auxiliary propulsion, higher propulsion efficiency than traditional propellers can be expected. Though the duct may create more blockage to the rotor wake, it protects the propeller from excessive propeller/rotor aerodynamic interactions. If mounted at the wing tip, to form a tilt-ducted-fan configuration such as the Doak VZ-4, the ducted fan produces less wing downwash. The duct also provides protection to the propeller, and to ground personnel/equipment. Especially in emergencies, the duct can support containment, preventing further damage to the airframe. Further, by adding guide vanes at the outlet to deflect the airflow, the ducted fan is able to provide vectored thrust either for sideways propulsion or control purposes, hence, in several cases, the need for tail rotor and empennage can be eliminated, as in the Piasecki 16H-1A (see Fig. 1(a)). A future ducted fan could be made into a compact, electricity-driven, removable, plug-in, propulsion unit, by integrating the control and power inside the shroud and introducing contra-rotating fans to eliminate the overall torque. This approach to design is important for the standardisation and modularisation of propulsion units for future novel rotorcraft configurations.

Indeed, a ducted fan can be made into an UAV if adequate, controlled, outlet vanes are added. Applications in propulsors for hovercraft, fan-in-wing configurations, or tail-rotor, as the fan-in-fin design for helicopters can also be found. Applications to marine propulsion,<sup>(9)</sup> and wind turbines<sup>(10,11)</sup> have also been reported. Nevertheless, few compound helicopters have adopted ducted fans for propulsion, e.g. the Piasecki 16H-1A (Fig. 1(a)) and X-49A (Fig. 1(b)), and the VFW H3 Sprinter (Fig. 1(c)). In Johnson's conceptual design for urban compound helicopters,<sup>(12,13)</sup> ducted fans were chosen for efficiency and safety reasons,

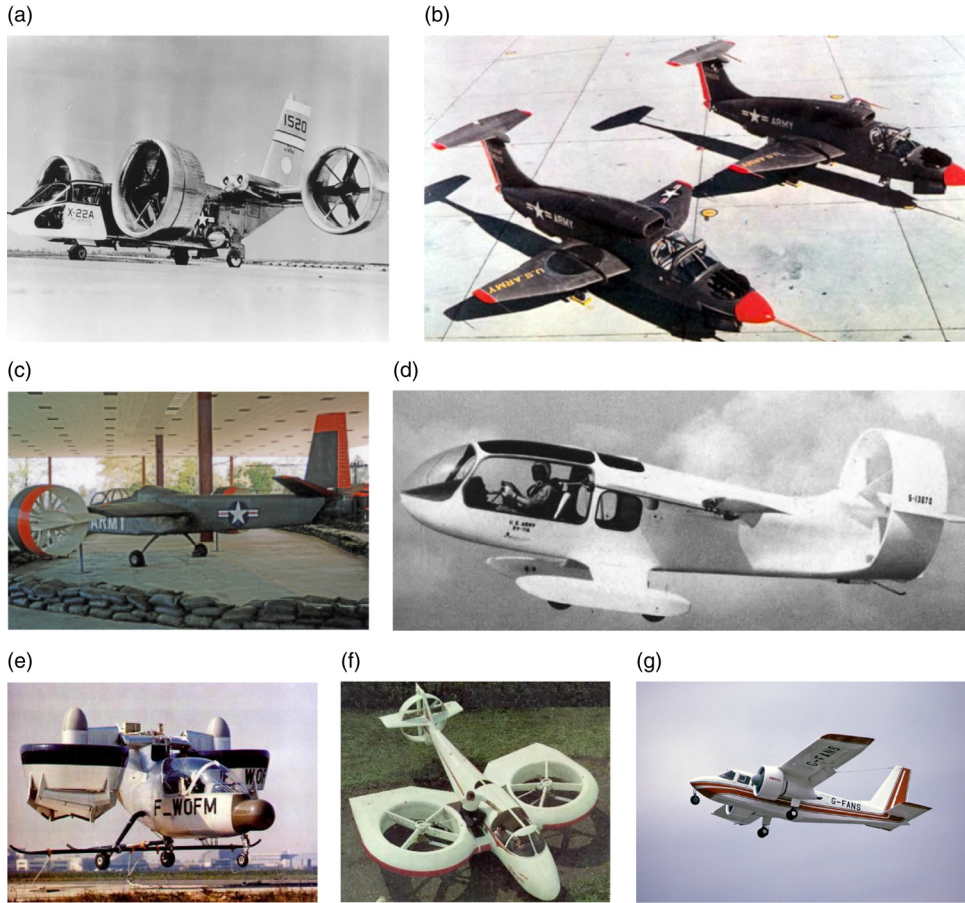


Figure 2. Ducted fan aeronautical implementations (20<sup>th</sup> century). (a) Bell X-22A. (b) Ryan XV-5. (c) Doak VZ-4. (d) XV 11A Marvel. (e) Nord 500 Cadet. (f) Vanguard Omniplane. (g) Britten-Norman BN-2 Islander.

and were mounted on wings near the tail, under the rotor (Fig. 1(d)). However, very few performance analyses of the ducted fans in these configurations can be found in the open literature. More applications of ducted fans are presented in Fig. 2(a)–(g), such as on the Bell X-22A aircraft (Fig. 2(a)) and the Doak VZ-4 (Fig. 2(c)). More recent applications are shown in Fig. 3(a)–(e), such as on the Hybrid Air Vehicle (Fig. 3(b)) and the Airbus E-fan (Fig. 3(d)). The recently unveiled Bell Nexus air taxi, as shown in Fig. 3(e), features six tiltable ducted fans for lift and thrust. However, it should be noted that most of these aircraft were prototypes and did not enter production, or service.

The disadvantages of a ducted fan, in comparison to an open propeller, apart from the salient weight and drag penalty due to the shroud, include poor performance at very high duct angles of attack, inflow distortion and possible stall on the upstream inner duct side. This can possibly be triggered by high-rate descending or working under substantial downwash flow. Aerodynamic forces and moments imposed on the duct may also be problematic. However, the aforementioned benefits may still give the ducted fan a chance to compensate



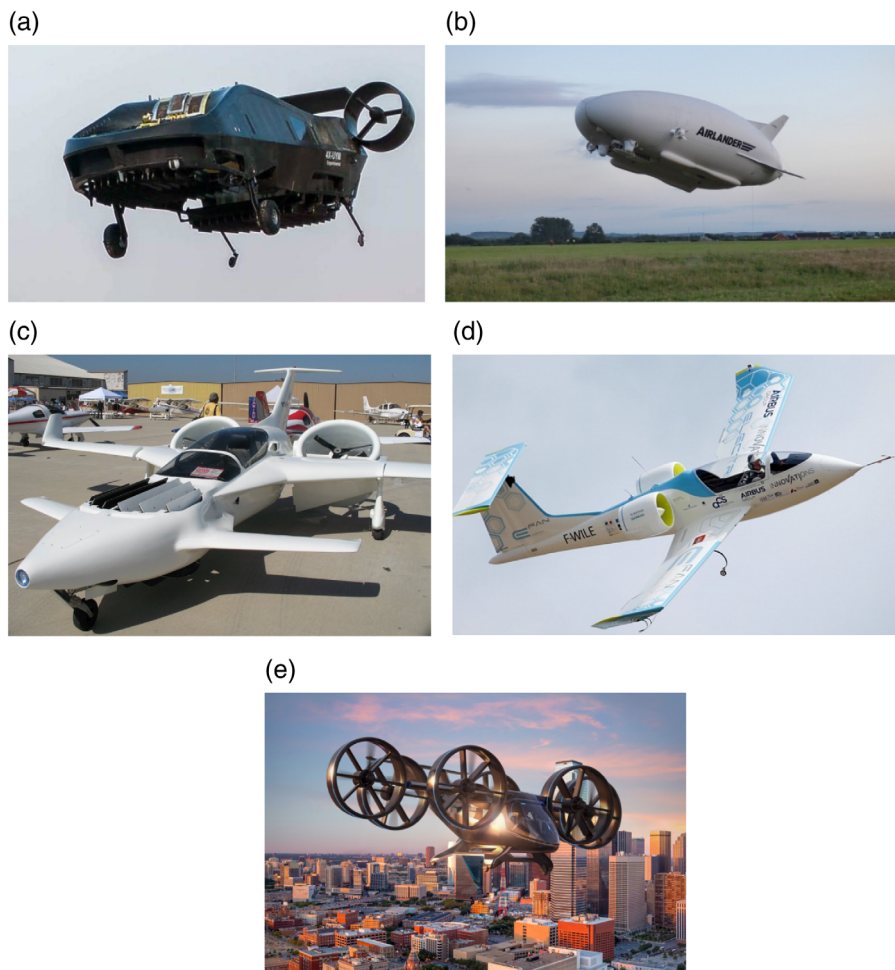


Figure 3. Ducted fan aeronautical implementations (21 st century). (a) UrbanAero AirMule. (b) Hybrid Air Vehicle. (c) Parker Alienair 1. (d) Airbus E-fan. (e) Bell Nexus.

for its deficiencies. Treatments and optimisation to mitigate the deficiencies should be further investigated and evaluated in future ducted fan research.

## 2 EXPERIMENTAL WORKS ON DUCTED FANS

As summarised by Sacks and Burnell,<sup>(2)</sup> Pereira<sup>(3)</sup> and Akturk and Camci,<sup>(4)</sup> plenty of experimental and theoretical studies on ducted fan aerodynamics can be found. Recent experimental studies mostly focused on UAV/MAV applications. Therefore, as shown in Figs 4 and 5, the scale, compressibility, and Reynolds number (based on free-stream speed and duct chord length) of recent studies are only comparable to small, model-sized experiments from years ago. As suggested by Goodson and Grunwald,<sup>(14)</sup> model-sized tests can be used to approximate full-scale performance, provided that the duct lip separation effects are avoided. However, lip separation is more likely to take place in model-sized tests due to the low Reynolds number. Table 1 presents a summary of the experiments, including the model

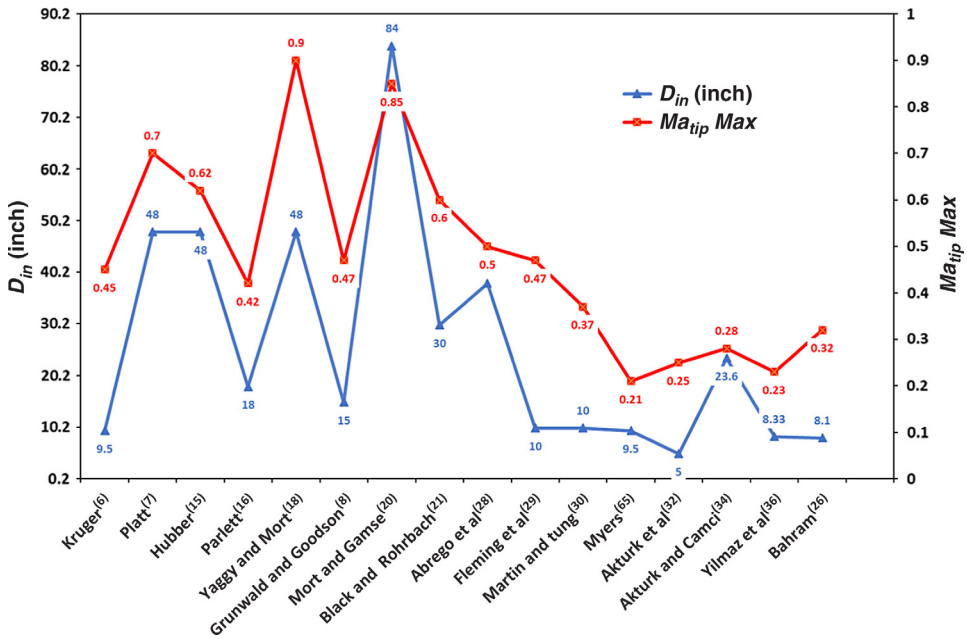


Figure 4. Scale (denoted by duct inner diameter  $D_{in}$  in *inch*) and compressibility (denoted by maximum blade tip Mach number  $Ma_{tip Max}$ ) comparisons of ducted fan experiments.

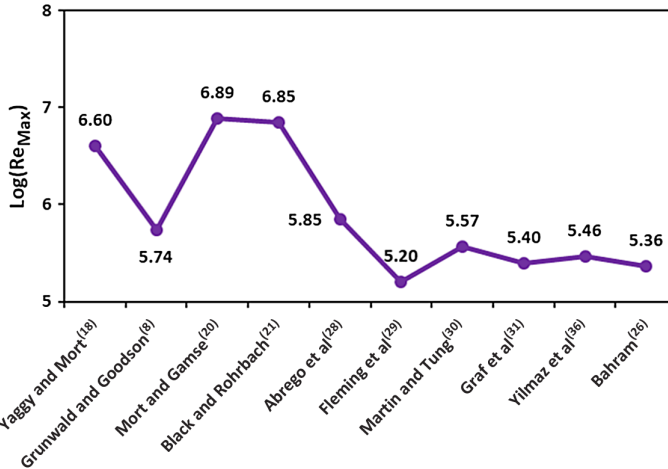


Figure 5. Maximum Reynolds number comparisons of ducted fan experiments (based on  $V_{\infty}$  and  $c_{duct}$ ).

scales and geometries, estimated maximum tip Mach number, and main objective of each study. These experiments are discussed in detail in this section, with emphasis put on studies featuring large duct sizes, high Reynolds numbers, and well-documented setups.

### 2.1 Early experiments on ducted fans

Selected early experiments are listed in Fig. 6(a)-(k). Very early experiments before the 1960s (Fig. 6(a)-(e)) are summarised briefly in Table 1 due to lack of detailed information in the

**Table 1**  
**Experiments on ducted fans**

<b>Case</b>	$c_{duct}$ (inch)	$D_{in}$ (inch)	Max $Ma_{tip}$	Duct GEO	Centre-body GEO	Blade GEO	Vane GEO	Recommended for numerical validation	Note
Kruger <sup>(6)</sup>	1.482–10.45	9.5	0.45	A (img)	A	A	NA	N	Various duct shapes and propellers
Platt <sup>(7)</sup>	32.2–40.1	48	0.7	A	NA	A (nbs)	–	N	Dual-rotating rotors
Hubbard <sup>(15)</sup>	9.6–28.8	48	0.62	A	NA	A	–	Y	Acoustic study
Parlett <sup>(16)</sup>	12.25	18	0.42	A (img)	NA	NA	–	N	–
Taylor <sup>(17)</sup>	0.48–16.48	16	NA	A	NA	A	–	N	Fan in wing configuration
Yaggy and Mort <sup>(18)</sup>	33	48	0.9	A	A	A (nbs)	A	Y	VZ-4 ducted fan
Grunwald and Goodson <sup>(8)</sup>	10.312	15	0.47	A	A	A	–	Y	$AoA$ study
Mort and Gamse <sup>(20)</sup>	49	84	0.85	A	A	A (nbs)	A	Y	X-22A ducted fan
Black and Rohrbach <sup>(21)</sup>	20(15)	30	0.6	NA	NA	NA	NA	N	Comprehensive study

**Table 1**  
**Continued**

Case	$c_{duct}$ (inch)	$D_{in}$ (inch)	Max $Ma_{tip}$	Duct GEO	Centre-body GEO	Blade GEO	Vane GEO	Recommended for numerical validation	Note
Abrego et al. <sup>(28)</sup>	10	38	0.5	NA	NA	NA	NA	N	PAV ducted fan
Fleming et al. <sup>(29)</sup>	6	10	0.47	NA	NA	NA	NA	N	Control methods study
Martin and Tung <sup>(30)</sup>	5.77	10	0.37	A (img)	NA	NA	–	N	Panel method validation available
Graf et al. <sup>(31)</sup>	5	10(11.25)	NA	NA	NA	NA	–	N	Lip shape and control methods study
Akturk et al. <sup>(32)</sup>	NA	5	0.25	NA	NA	NA	–	N	PIV measurements
Ohanian et al. <sup>(66)</sup>	NA	NA	NA	NA	NA	NA	–	N	Synthetic jet
Akturk and Camci <sup>(34)</sup>	NA	23.6	0.28	A	NA	A	–	N	Tip clearance study
Rhee et al. <sup>(35)</sup>	4.65	9.5	0.21	NA	NA	A (nbs)	–	N	Acoustic study
Yilmaz et al. <sup>(36)</sup>	8.33	8.33	0.23	A	NA	NA	–	Y	Pressure and velocity field measured
Bahram <sup>(26)</sup>	8.66	8.1	0.32	NA	NA	NA	NA	Y	Asymmetric duct

A: Acquirable, NA: Not Acquirable. img: geometry provided by images. –: not included. nbs: no blade sections available

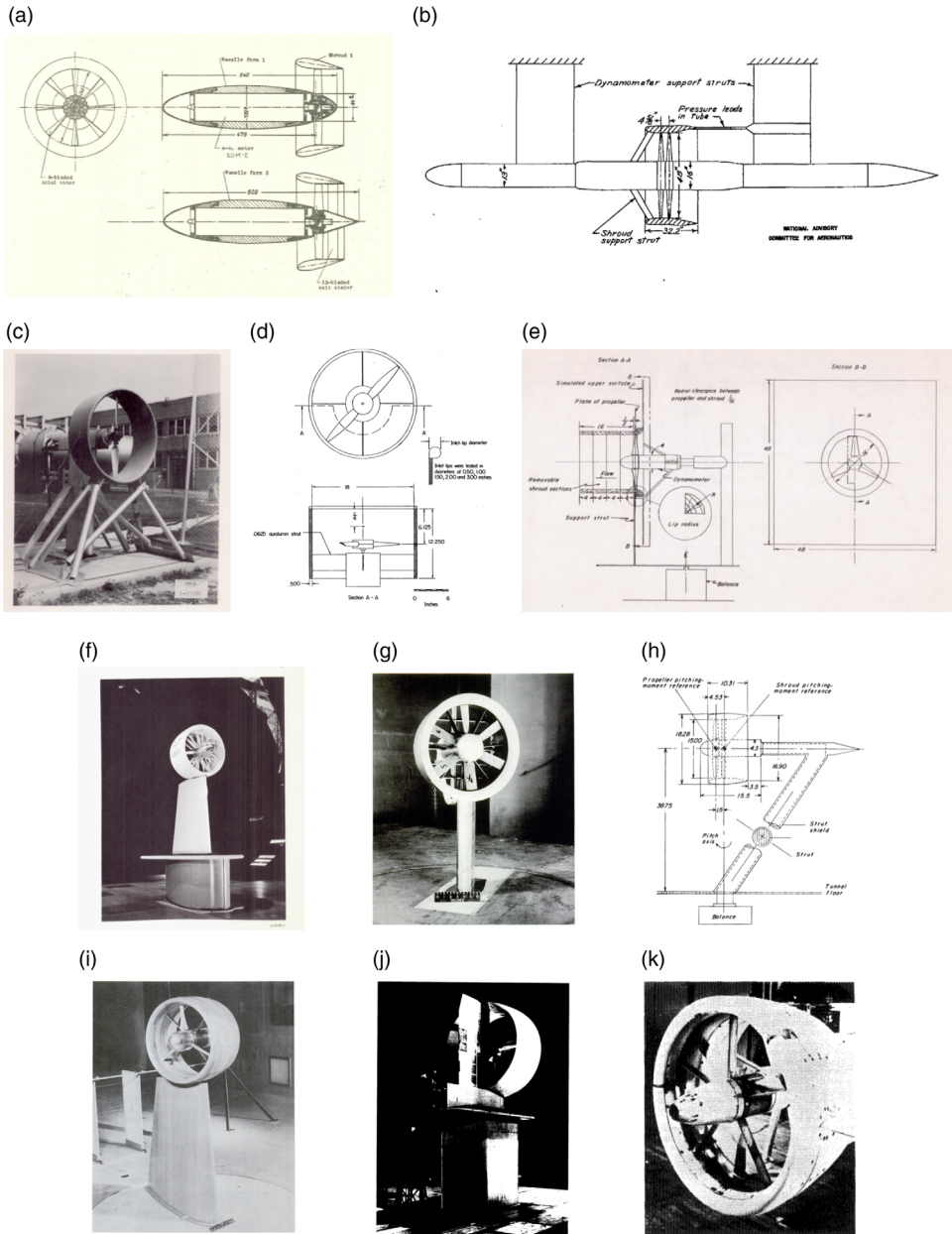


Figure 6. Early experiments on ducted fans. (a) Krüger.<sup>(6)</sup> (b) Platt.<sup>(7)</sup> (c) Hubbard.<sup>(15)</sup> (d) Parlett.<sup>(16)</sup> (e) Taylor.<sup>(17)</sup> (f) Yaggy and Mort.<sup>(18)</sup> (g) Grunwald and Goodson.<sup>(19)</sup> (h) Grunwald and Goodson.<sup>(8)</sup> (i) Godson and Grunwald.<sup>(14)</sup> (j) Mort and Gamse.<sup>(20)</sup> (k) Black and Rohrbach.<sup>(21)</sup>

corresponding references. Nevertheless, results and conclusions of these tests are discussed in the summary of research challenges (Section 4). This section focuses mostly on the full-scale wind tunnel test campaign performed by NASA (Fig. 6(f-j)) during the development of two VTOL aircraft, the Doak VZ-4DA and the Bell X-22A, which utilised ducted fans for



propulsion and lift. The experiments focused on examining the aerodynamic performance of the specific designs. Test matrices of these experiments are presented in Tables 2–4.

The 4-foot-diameter ducted fan of the Doak VZ-4DA tilt-duct VTOL airplane was tested while mounted at the tip of a semi-span wing representing a real-world design (Fig. 6(f)). Experiments were systematically conducted and documented<sup>(18,22–24)</sup> to investigate the performance of this specific shape. It is noted that geometric information of the entire wing/ducted-fan combination was presented in detail, except for the blade sections. The configuration had a complex structure, as the propeller was eight-bladed. A nine-bladed stator was installed to support the centre-body. Either 7 or 14 guide vanes were installed at the duct inlet, and a small tapered wing with a 25% plain flap was placed at the exit as a guide vane.

The experiments accounted for comprehensive variations including free-stream speed,  $AoA$  of the wing, the ducted fan's relative angle to the wing, advance ratio, blade pitch angle, power input etc. Power, forces and moments of the ducted fan and wing combination, stall boundary for the upstream lip (through tuft flow visualisation), and surface pressure were measured. To support future use of the ducted fan for control purposes, the effectiveness of various means, i.e. inlet vanes to alter the effective pitch angle of the blades, direct change of the blade pitch, and exit vanes to deflect the air, were evaluated. The exit vane was eventually concluded as the most effective method. In these full-scale tests, the maximum Reynolds number based on the free-stream speed and the duct chord length was between 4 and 7m. The experiments, however, did not provide comprehensive measurements of the isolated ducted fan (though the isolated wing's performance was measured), as the duct had to be mounted at the wing-tip.

Grunwald and Goodson<sup>(14,19)</sup> also tested two model-sized wing/ducted-fan combinations (Fig. 6(g) and (i)), to investigate the aerodynamic characteristics in hover and transition modes. It was found that the ducted propeller carries a substantial proportion of forces during hovering and transition modes, and causes a large nose-up moment at low speed. With the exit guide vanes, the forces and moments could be trimmed, effectively. However, due to the small scale of the models and the resulting low Reynolds numbers (around 0.5m), flow separation at the duct lip, which at full-scale may not be present, could not be avoided. Both experiments documented the geometry and the test conditions, but the propeller blade sections were not mentioned. However, it should be noted that, though not stated explicitly in the documents, the same ducted fan model was apparently used for the wing/ducted-fan combination study<sup>(14)</sup> and to study cross-wind effects<sup>(8)</sup> (Fig. 6(h)), and the blade sections are reported in Ref. [8]

Later, a Bell X-22A ducted fan was examined by Mort and Gamse<sup>(20)</sup> in the NASA Ames 40- by 80-foot wind tunnel during the aircraft development (Fig. 6(j)). Along with the aforementioned 4-foot experiments, the test was summarised by Kriebel and Mendenhall.<sup>(25)</sup> Theoretical models were then built and examined. The models could predict well the ducted fan performance, yet differences could not be avoided due to the unevenly distributed disk loading and flow separation, showing the need for high-fidelity analyses.

Geometric definitions of the duct and the vanes were presented as well, but the blade profile was not documented. The structure of the 7-foot-diameter ducted propeller was slightly simpler than the 4-foot one of Ref. [18]. The duct was 49 inches in length, and had six unevenly distributed stator blades to support the centre-body. A three-bladed propeller was employed. A guide vane, similar to a small wing of rectangular planform, was installed at the flow exit to deflect the exhaust. Aerodynamic forces, power, and moments of the isolated ducted fan were measured, excluding the contributions from the wind tunnel support structure and fairing. Free-stream dynamic pressure, blade pitch angle, rotor RPM,  $AoA$  of the duct, and the exit vane deflection angle were set as the variables. The maximum Reynolds number based

**Table 2**  
**Test matrix for the 7-foot ducted fan by Mort and Gamse<sup>(20)</sup>**

<b>Variations</b>	<b>Free-stream dynamic pressure (psf)</b> <b>0–106</b>	<b>RPM</b> <b>1,200– 2,590</b>	$\mu$ <b>0–2.2</b>	<b>AoA (deg)</b> <b>0</b>	<b>Vane deflection (deg)</b> <b>Off/–17 to +20</b>	$\beta$ (deg) <b>14–49</b>	<b>Static thrust coefficient<sup>(20)</sup></b> –	<b>Emphasis</b> –
Case 1	NA	NA	0–22	0	Off/0	14–49	–	Static perfor- mance
Case 2	NA	1,810–2,590	NA	0–90	Off/–17 to +20	14, 19, 29	5.0–28.7...	AoA
Case 3	10.2–67.7	–	–	0–90	0	–	–	Duct alone
Case 4	0, NA	NA	–	0	–20 to 20	19	NA/0.4– 13.5	Vane effec- tiveness
Case 5	NA	1,806	–	30–80		19	5.0	Stall boundary

**Table 3**  
**Test matrix for the 4-foot ducted-fan/wing combination by Yaggy and Mort<sup>(18)</sup>**

<b>Variations</b>	$V_{\infty}$ (knots) <b>0–140</b>	<i>RPM</i> <b>&lt;6,600</b>	AoA_wing (deg) <b>0–20</b>	AoA_duct (deg) <b>0–90</b>	Vane deflection (deg) <b>0–30/0–20</b>	<b>Emphasis</b> –
Case 1	NA	Windmill	0–20/0	0/0–90	Off	Static performance
Case 2	0–140	3,600–4,800	2, 6	0–90	Off	Force balancing
Case 3	20–50	3,600–4,800	2, 6	Balance conditions	Off, 0, 10, 20, 30/0 10/20	Exit vane effectiveness
Case 4	0–140	3,600–4,800	2, 6	40–80	Off, 0, 10, 20, 30/0 10/20	Force balancing exit vanes

**Table 4**  
**Test matrix for the 5/16 model-sized ducted fan by Grunwald and Goodson<sup>(8)</sup>**

<b>Variations</b>	$V_\infty$ (ft/s)	<b>RPM</b>	<b>AoA</b> (deg)	$\beta$ (deg)	$\mu$	<b>Lip</b> <b>modification</b>	<b>Emphasis</b>
	–	<b>8,000</b>	<b>–10 to 110</b>	<b>24</b>	<b>0–0.595</b>	<b>On/off</b>	–
Case 1	100	Removed/ windmilling	0–100	24	–	On/off	Power-off
Case 2	–	8,000	0–110	24	0–0.595	On/off	AoA

on the length of the duct was around 13m. However, only dimensionless parameters for the test conditions were documented, making the determination of the specific conditions difficult. Pressure distributions inside and outside the duct surfaces were also provided. The experiments confirmed the high performance of the specific design, and concluded that better high-speed performance could be achieved with design modifications. Pressure distribution measurements were included to identify stall at inlet and outlet. The geometry and stall boundary of the 7-foot duct were similar to those of the 4-foot duct.<sup>(18,22–24)</sup> It was also found that upstream lip stall could easily happen at low power and high duct angle conditions, but stall at the downstream lip was not likely. Initially, the separation was local, and no large changes in performance were observed. As the cross-wind angle increased, flow separation occupied the entire duct lip and large changes in aerodynamic loads were noticed. The authors claimed that there is a critical lip radius above which the flow separation would be delayed and vice versa. In general, it can be argued that the duct lip separation depends on the difference between the fan power and the free-stream speed, the cross-wind angle, and the inlet lip geometry.

Experimental, and theoretical studies on more general configurations were also conducted. Black and Rohrbach<sup>(21)</sup> systematically investigated the performance of a 3-foot ducted fan, considering geometric variations of expansion ratio, inlet lip shape, external duct shape, propeller location, inlet/outlet vanes, blade shape, blade number, tip speed, and tip clearance (Fig. 6(k)). The Mach number varied from 0.2 to 0.6 and comparisons were made against open propeller counterparts, with contributions from the duct and the propeller measured separately. Cross-wind effects were not included, but this research represents a comprehensive experimental investigation into the dominant factors of the ducted-fan static performance. The expansion ratio was identified as the most critical factor, which was consistent with theoretical analyses. A larger expansion ratio would be more beneficial to the static performance, but the cruise performance might be compromised. The authors recommended either specific shape optimisation or deformable shapes, as a way forward.

To study cross-wind effects, Grunwald and Goodson<sup>(8)</sup> conducted experiments on a 15-inch diameter ducted fan, representing a 5/16 model of the aforementioned 4-foot ducted fan (Fig. 6(h)), considering duct AoA ranging from  $-10^\circ$  to  $110^\circ$ . No inlet nor outlet guide vanes were installed. The maximum Reynolds number, based on the tunnel wind speed and the duct length, was around 0.5m, corresponding to forward flight transition conditions of a tilt-duct VTOL aircraft. Shroud lip separation was identified as the angle-of-attack increased. The experiments also uncovered that the propeller contributions to the overall forces and moments were relatively small, highlighting the importance of the duct. Also, at different advance ratios, as long as separation appeared, the ratio of the propeller thrust to the total thrust grew rapidly. This ratio, however, decreased with the duct AoA when stall was eliminated, suggesting that stall has a detrimental effect on the duct's performance. It is interesting

that a modified lip geometry was proposed to resolve lip stall, and was shown to be effective. This suggests that an asymmetric duct design may be necessary, as also investigated by Bahram.<sup>(26)</sup> However, it should be pointed out that the stall boundary specified by this model-sized experiment is narrower than the full-scale experiments. The scale of the duct plays an important role in the stall characteristics. As concluded by Mort,<sup>(23)</sup> for ducted fans that are big enough, e.g. those utilised by the X-22A and the VZ-4, inlet lip stall can only be encountered at very high rates of descent. The reports provided detailed geometric information about the blade and the duct, hence numerical validation can be made. In particular, Xu et al.<sup>(27)</sup> simulated the experiment at the  $AoA$  of  $50^\circ$  using RANS. The stall on the upstream side was predicted and visualised, then a modified lip shape was added to eliminate the stall. Very limited data comparisons were made; nonetheless good agreement was achieved.

## 2.2 Recent experimental studies

A resurgence of ducted fan research in industry started in the 2000s because of the growth of interest in UAVs, PAVs, and electric propulsion. The models used in more recent experiments are presented in Fig. 7(a)–(k). Recent efforts feature a combination of modern experimental technologies and CFD simulations. However, it is noted that the scale of the models examined, and the resulting Reynolds numbers and compressibility were hardly comparable to experiments from the 1960s, as the recent research targeted mostly small-scale UAVs (such as in Fig. 7(b), (e), (g) and (i)). These studies often utilised very high RPM rotors (typically more than 8,000 RPM) at low Reynolds number ( $10^4$ – $10^5$ ). Such combinations do not represent high-speed flight conditions, and can hardly be applied to large aircraft. Nevertheless, the tests are briefly summarised in Table 1, and some are further discussed in Section 4. Few experiments utilised large-scale models and/or presented inspiring results for aircraft applications, and these are summarised in detail.

Abrego and Bulaga<sup>(28)</sup> investigated a ducted fan designed for PAVs. The ducted fan, as shown in Fig. 7(a), had a duct inner diameter of 38 inches and a 10-inch duct chord. A five-bladed propeller was installed. Two 3-inch exit guide vanes were used to vectorise the flow. The experiments accounted for various tunnel speeds,  $RPM$ ,  $AoA$ , and vane deflection angles. The data and geometry were later adopted for CFD validation by Chang and Rajagopalan.<sup>(37)</sup> The simulated results matched the corrected experimental data, though the fan was represented by momentum sources. However, the detailed geometric information is not publicly available. Martin and Tung<sup>(30)</sup> examined a two-bladed, 10-inch ducted fan UAV (Fig. 7(c)), taking into account variations of the tunnel velocity,  $AoA$ ,  $RPM$ , tip clearance, and duct leading edge radius. The performance of the ducted fan, as well as, of the isolated propeller, were measured. Stall boundaries of the isolated duct and the powered configuration were also identified. It was found that increasing the tip gap would severely compromise the overall performance. The experiments also reported that the flow appeared to separate after the rotor blade plane. The ducted fan model utilised in the tests was simple, and its purpose was to provide validation data for future modelling. However, the geometry of the duct and the blade, including the location of the propeller, are not explicitly defined in the paper. The experiments were later compared against panel method calculations by Lind et al.,<sup>(38)</sup> and good correlation within the attached flow region was achieved.

Akturk and Camci<sup>(4,34,39–41)</sup> and Akturk et al.<sup>(32)</sup> carried out numerical and experimental studies on ducted fan UAVs. They used PIV to measure the flow field outside a small ducted fan model<sup>(32,40)</sup> (Fig. 7(f)), and the measurements agreed well with CFD simulations, where the rotor was represented by an actuator disk. The inlet flow distortion in conditions was



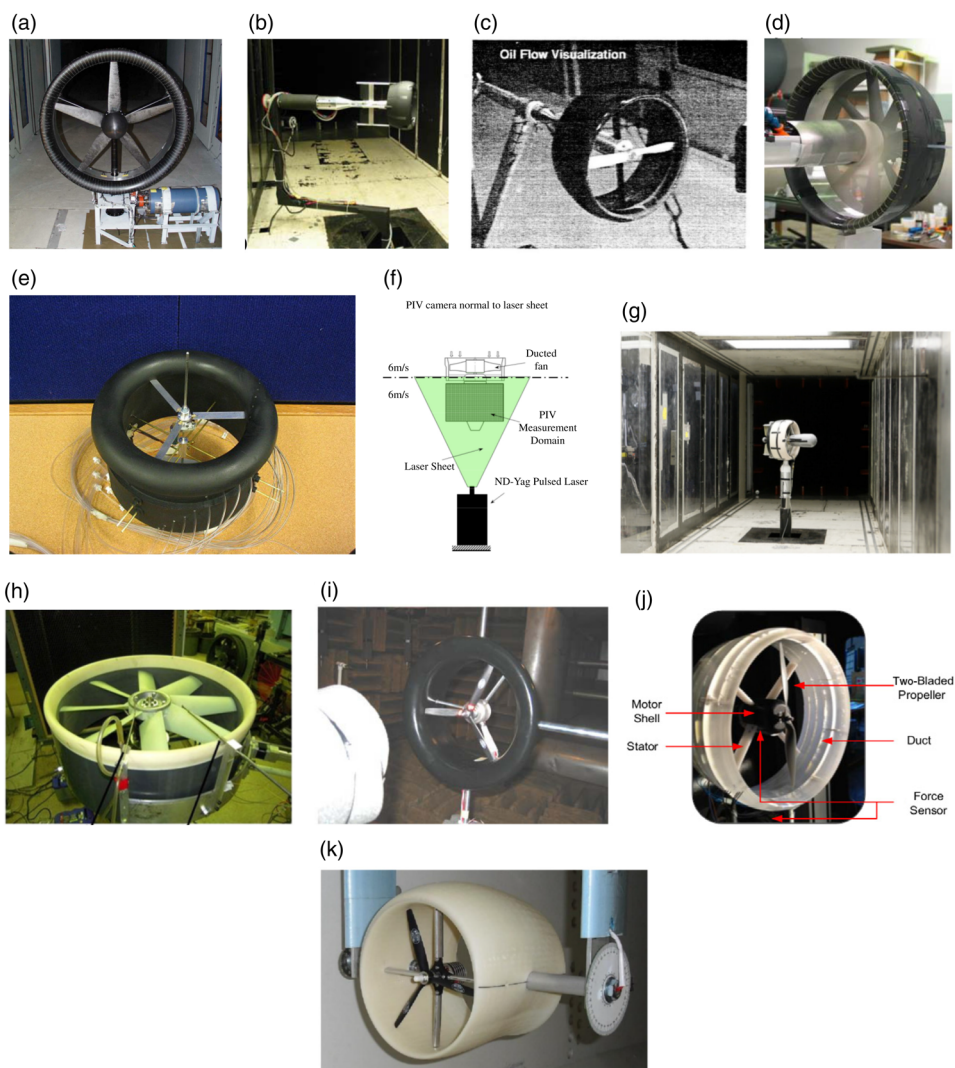


Figure 7. Recent experiments on ducted fans. (a) Abrego et al.<sup>(28)</sup> (b) Fleming et al.<sup>(29)</sup> (c) Martin and Tung.<sup>(30)</sup> (d) Graf et al.<sup>(31)</sup> (e) Pereira.<sup>(3)</sup> (f) Akturk et al.<sup>(32)</sup> (g) Ohanian et al.<sup>(33)</sup> (h) Akturk and Camci<sup>(34)</sup> (i) Rhee et al.<sup>(35)</sup> (j) Yilmaz et al.<sup>(36)</sup> (k) Bahram.<sup>(26)</sup>

revealed. However, due to the geometry of the duct, the flow field inside it, and near the blades could not be captured by the experiments. The free-stream speed was only 6m/s while the rotor *RPM* reached 9,000, which is typical for the ducted fan UAV studies as mentioned earlier. This is one of the few studies that first employed commercial codes and examined their applicability for ducted flow simulations. Later, Akturk and Camci also employed CFD methods in their double ducted fan<sup>(4,39)</sup> and tip clearance studies (Fig. 7(h))<sup>(34,41)</sup>.

More recently, Yilmaz et al.<sup>(36)</sup> examined five different circular duct shapes using the same two-bladed propeller and a constant *RPM* (Fig. 7(j)). The duct sections were defined by several standard NACA airfoils or their combinations. The duct inner radius and the chord length were kept at 0.2117m, while the free-stream speed was up to 25m/s. The resulting Reynolds number

based on the chord length was around half of Grunwald's experiment. The blade geometry, however, was not described in detail. Performance of the open propeller was measured at different advance ratios for the purpose of further comparisons. The tests mainly explored effects of the advance ratio and the duct shape on the overall performance, and found that as the advance ratio grows, the thrust coefficient decreases and eventually becomes negative. A duct shape that has higher profile camber and higher expansion ratio was shown to provide better performance in the test. Also, the experiments showed that the propeller inside the duct performs poorer than the open propeller, but the overall performance of the ducted fan is better. Apart from force and power coefficients, the velocity profiles at the inlet and exit were measured and the results were presented. Pressure distributions along the duct inner surface were presented too. This case is suited for CFD validation despite the low Reynolds number, since the duct geometry is simple, the propeller can be represented by a matched model, and the available measurements are quite elaborate.

As most studies focused on the global shape, or the aft shape of the duct, Graf et al.<sup>(31)</sup> specifically studied the inlet lip (Fig. 7(d)). The study pointed out that the lip shape defines the lip suction effect and alters the location of the pressure centre, which will further affect the pitching moments. Four different lip shapes were tested at static and cross-wind conditions. It is found that an increased lip radius is beneficial for static performance, due to its ability to maintain attached flow longer. However, the profile drag and the pitching behaviour brought by the lip shapes were detrimental. Compromise should therefore be made between the best static and best cross-wind performance. It is also interesting that the two symmetric shapes tested, showed poorer static performance, while shapes that generate a larger suction area in the inner surface were more favourable. Nonetheless, the experiments aimed at UAV applications, and the Reynolds number was low. Information on the model geometry and the detailed performance data was also restricted.

## 3 MODELLING DUCTED FANS

### 3.1 Theoretical and low-order methods

Theoretical studies on ducted fan performance using methods like the annular airfoil theory, lifting line, blade element or panel methods etc. can be found in the literature since many decades ago. Thwaites<sup>(42,43)</sup> presented detailed analyses for a fan inside a duct or tunnel based on strip theory, in the early 1950s. Kriebel and Mendenhall<sup>(25)</sup> compared their theoretical analyses against experimental data, though in many cases, where heavy disk loadings and flow separation were encountered, only qualitative agreement could be achieved. Pereira<sup>(3)</sup> also presented a detailed theoretical study. More recently, Bontempo and Manna<sup>(44)</sup> studied the exact solution of incompressible, axisymmetric and inviscid flow through the duct enclosing a non-uniform actuator disk. These methods can rapidly and quite accurately predict the performance in simple cases, and are suitable for fast analysis, of preliminary designs, for parametric studies.<sup>(45)</sup> However, in many cases, especially where flow separation is encountered, such models can only deliver results in qualitative agreement with test data.

Ahn and Lee<sup>(49)</sup> proposed an axisymmetric analysis and design method for ducted fans, based on the extended stream-surface method by Ahn and Drela.<sup>(50)</sup> Viscous effects were not included. The study investigated the diffuser angle and inlet lip radius, as well as it compared fan disk models, and tip loss models, but no validation was provided. The duct expansion angle was found to be the dominant factor, as also suggested by many previous studies.

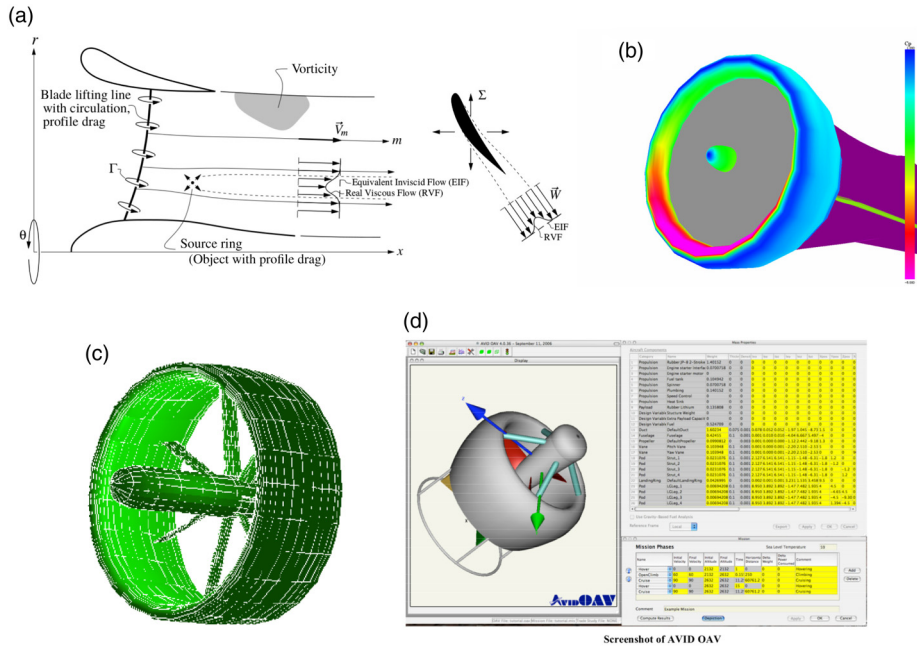


Figure 8. Lower-order simulations of ducted fan flow. (a) DFDC (Ducted Fan Design Code)<sup>(46)</sup> (blade elements, lifting line, panel methods). (b) Lind et al.<sup>(38)</sup> (blade elements, panel methods). (c) Bi et al.<sup>(47)</sup> (blade elements, panel methods). (d) AVID OAV<sup>(48)</sup> (empirical data interpolation, actuator disks).

The inlet radius was shown to be less important. However, as evidenced by the experiments reported by Talyor,<sup>(17)</sup> smaller lip radii may give rise to inflow separation at the lip. The computational resources required for the aforementioned analyses were very small. Later, an open source code called DFDC (Ducted Fan Design Code) by Youngren et al.<sup>(46)</sup> and Dreila and Youngre<sup>(51)</sup> was also reported (Fig. 8(a)). The code calculates rotor(s) using a lifting-line representation, blade element models, and vortex sheets, while the duct and centre-body are accounted for using axisymmetric panel methods. The code is capable of rapidly predicting the performance of ducted fans that have multiple rows of rotors and stators. It is also capable of quick design of ducted fans given certain performance requirements. DFDC can be found deployed in several analysis and design studies, but its accuracy is not widely validated. In addition, the code can only account for axial flight and steady conditions.

Lind et al.<sup>(38)</sup> adopted panel, as well as, blade element methods based on airfoil tables to model the Martin and Tung's experiments<sup>(30)</sup> for a 10-inch-diameter ducted rotor. The potential flow method (Fig. 8(b)) predicted the forces well at high rotor *RPM* (9,000) and low free-stream speed, for *AoA* up to 90°. However, the discrepancies in the pitching moment results were stronger. It is also noted that no lip separation occurred. At high free-stream speeds, only low *AoA* cases were compared. Nevertheless, the method required very low computational resources, and was seen as suitable for preliminary analyses. Bi et al.<sup>(47)</sup> investigated ducted fans designed as aerodynamic propulsors for shipboard applications using panel methods for the duct frame, and blade element methods for the propeller (Fig. 8(c)). The simulations, investigated the effect of variables including advance ratio, compressibility, blade twist, propeller location, and tip clearance. The study showed a decrease of the duct

thrust contribution as the advance ratio increased. The inlet blockage was also investigated, and was found that it may induce significant vibration on the fixed and rotating parts of the structure. Validation was made against experiments, however, due to the proprietary nature of the model, quantitative comparisons were not publicly available.

The above mentioned methods can effectively and quickly calculate static performance, but can hardly account for flow separation and arbitrary flight conditions. Hence their usage is limited, and corrections from tests may be necessary. Nonetheless, Ko et al.<sup>(48)</sup> presented a commercial code named AVID OAV (Fig. 8(d)), which integrates various strategies and multi-disciplinary methods. To predict and optimise performance of ducted fan UAVs, methods like interpolations from empirical data for duct performance, actuator disks or blade vortex element representations of the rotor, empirical equations for control vane performance, etc. were considered. The predictions were in good agreement with wind tunnel and flight test data, and the code has been used for several ducted fan UAV designs such as the iStar.<sup>(52)</sup> However, as mentioned above, the commercial code aimed at UAV applications, and little information is publicly available.

### 3.2 CFD simulations

The simulation of ducted fans, with blades and stators resolved, is within the capability of modern CFD methods and computers. Also, with the rapid development of commercial codes, many CFD simulations on UAV configurations were carried out in combination with practical tests. However, simulations of full-scale ducted fans for propulsion purposes at high Reynolds numbers are less common, and the same is true for ducted fans with stators or guide vanes. Simulation works are summarised here, as shown in Fig. 9(a)–(k), to show the advancements of CFD techniques, and suggest future development.

In early attempts, actuator disk models for the propeller and incompressible Navier–Stokes simulations were considered. Rajagopalan and Zhang<sup>(53)</sup> used steady and incompressible Navier–Stokes equations, and an axisymmetric reference frame to simulate propellers with and without a duct (Fig. 9(a)). The propeller was represented by a time-averaged momentum source term, which was defined by the blade geometry and sectional airfoils. However, the presented results failed to capture the pressure jump on the inner duct surface caused by the propeller. Only the propeller performance was presented, but no validation of the overall configuration was provided. Later, using similar methods, Chang and Rajagopalan<sup>(37)</sup> performed simulations and validated their results against the Abrego et al.<sup>(28)</sup> experiments. Though the fan was modelled by a momentum source and only axisymmetric conditions could be accounted for (Fig. 9(b)), good agreement with the corrected wind tunnel data was reported. Such combinations of actuator disks and incompressible governing equations is common and cost efficient, especially for fast analyses of UAV/MAV designs, but the axisymmetric restriction is usually prohibitive for more realistic situations. In addition, the disk models should be tuned with caution, as the thrust distributions on a propeller disk inside the duct differ considerably from that of an open propeller.

More CFD simulations with resolved propeller blades and compressibility effects accounted for, appeared recently. Akturk and Camci<sup>(4,34,41)</sup> conducted a series of combined experimental and numerical studies on double ducted fan designs and tip clearance. Their simulation included realistic blade shapes and various tip shapes (Fig. 9(c)). Validation, at low Reynolds numbers, proved that modern CFD methods are well-suited for ducted fan flows. The experiments by Grunwald and Goodson<sup>(8)</sup> were chosen for CFD validation by several researchers as shown in Fig. 9(d), (e) and (k). As mentioned earlier, Xu et al.<sup>(27)</sup> simulated the case at the  $AoA$  of  $50^\circ$  using the exact geometry and RANS methods (Fig. 9(e)). The stall



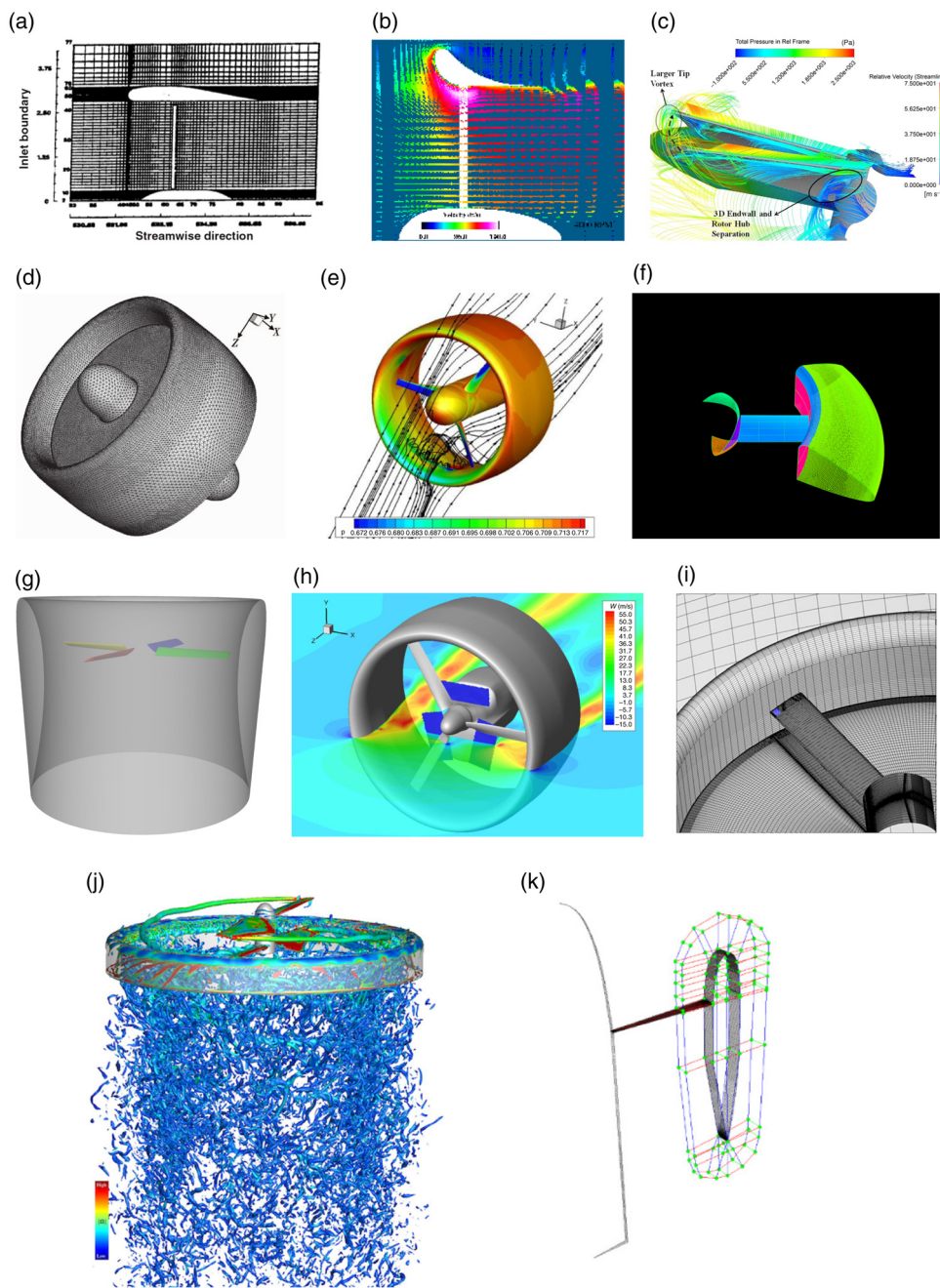


Figure 9. CFD simulations of ducted fan flow. (a) Rajagopalan and Zhang.<sup>(53)</sup> (b) Chang and Rajagopalan.<sup>(37)</sup> (c) Akturk and Camci.<sup>(34)</sup> (d) Ye et al.<sup>(54)</sup> (e) Xu et al.<sup>(27)</sup> (f) Sheng et al.<sup>(55)</sup> (g) Jimenez and Singh.<sup>(56)</sup> (h) Biava and Barakos.<sup>(57)</sup> (i) Chen et al.<sup>(58)</sup> (j) Rubio et al.<sup>(59)</sup> (k) Qing et al.<sup>(63)</sup>

on the upstream side was captured and visualised. Then, the modified lip shape was added and was shown to be effective in eliminating the lip stall. Though good agreement with the experimental data was achieved, very limited data was presented.



**Table 5**  
**Test matrix for the generic ducted fan simulations by Jimenez and Singh<sup>(56)</sup>**

	<i>RPM</i>	$\beta$ (deg)	$\mu$	Blade twist (deg)	Emphasis
Variations	1,500, 2,000	5, 10, 15, 19	0, 0.06, 0.11	-20, 0, 5	-
Case 1	1,500, 2,000	5, 10, 15, 19	-	-20, 0, 5	Hover
Case 2	1,500	19	0, 0.06, 0.11	0	Axial

**Table 6**  
**Test matrix of ducted fan tests by Yilmaz et al.<sup>(36)</sup>**

Duct shape	<i>RPM</i>	$V_\infty$ (m/s)	$\mu$	Tip clearance
NACA0018,0012,4312,+4312, M21+4312	7,000	0–25	0.08–0.4	0.038R

Sheng et al.<sup>(55)</sup> simulated a 24-inch diameter, six-bladed ducted fan in hover (Fig. 9(f)), representing a simplified fan-in-wing configuration. The study focused on examining effects of the blade twist and inlet lip radius. Comparisons between the ducted and open rotor configurations showed the higher efficiency of the ducted fan. The presence of the duct was also shown to delay the blade stall at high blade pitch angles. This was expected due to the flow acceleration at the duct lip. The influence of the blade twist was found to be consistent with open propeller cases. The inlet lip radius was shown to have significant impact on the hover efficiency, as a larger radius mitigates inlet lip separation. It was noticed that flow separation occurred at the lip, as well as downstream the blade disk at static conditions. The study detailed the geometry and test conditions, but relevant comparisons with experiments were not included. Numerical simulations by Jimenez and Singh<sup>(56)</sup> and Singh et al.<sup>(60)</sup> adopted a simplified and generalised geometry to study the ducted rotor aerodynamics through modern CFD methods (Fig. 9(g)). The test conditions and geometry were elaborately presented. The test matrix is shown in Table 5. The duct geometry from Mort's<sup>(23)</sup> experiments was used, but the propeller was replaced by a four-bladed simple rotor with the sectional profile of NACA23012. Another combination of a Clark-Y duct and NACA0015 blades was also tested. No centre-body was considered. Performance comparisons between the open and ducted counterparts were made in hover, at several rotating speeds, advance ratios and collective angles. Some performance gain at low advance ratio by the duct was observed. In their study, emphasis was put on propeller performance. It was found that due to the duct, the outer portions of the blades carried a higher fraction of thrust, while the inner parts were offloaded. Though no experimental validation was included, the study could be adopted for future experimental or numerical validation. However, some of the flow conditions tested show small shock waves on the blades.

More recently, Chen et al.<sup>(58)</sup> and Li et al.<sup>(61)</sup> modelled a tip-jet driven ducted fan design using URANS simulations, with the jet channel and the blade geometry resolved (Fig. 9(i)). Such a jet-driven design was used in lift-fan configurations like the Ryan XV-5 (Fig. 9(j)). This design has a simple structure and only a minor fraction of the fan's torque can be transmitted to the duct. The tip jet noise may, however, be substantial. Successful simulations of such a configuration demonstrated the capability of modern methods and computer

hardware. Very recently, Rubio et al.<sup>(59)</sup> carried out high-fidelity DDES (Delayed Detached Eddy Simulation) simulations for small-sized coaxial ducted rotors (Fig. 9(j)). The two-bladed rotor was scanned from a commercial quadcopter UAV. A high diameter-to-chord ratio duct was added. Complex flow features were resolved in detail. However, it was noticed that the duct chord was so short that it could barely cover the coaxial rotors. The simulations showed, for both single-rotor and coaxial configurations, the tip vortices were restricted by the duct. The pressure fluctuations were also altered by the duct, suggesting future use of the duct for acoustics control and reduction.

### 3.3 Optimisation studies

While most simulations focused on validation or performance analysis, design optimisation based on CFD methods has also been attempted. Schaller<sup>(62)</sup> developed an optimisation framework for small-scale ducts, based on a genetic algorithm coupled with simplified CFD simulations using momentum sources. The optimisation was shown to be effective for single-rotor and coaxial ducted fans, but the results lacked support from practical tests. Ye et al.<sup>(54)</sup> (Fig. 9(d)) applied global optimisation methods, based on response surfaces and neural networks, to Grunwald and Goodson's<sup>(8)</sup> duct. The static thrust generation was improved by about 20%, but the validation using the static case showed considerable discrepancy with experiments. Steady actuator disks instead of realistic blades were adopted for the flow calculation, and performance at higher advance ratios was not examined. Very recently, the same optimisation case was revisited by Qing et al.<sup>(63)</sup> (Fig. 9(k)) using similar but more detailed methods. It is very interesting to notice that the authors replicated the hover tests by Grunwald and Goodson<sup>(8)</sup> using the same duct and blade geometry, though they used variable *RPM* from 2,000 to 8,000. At the same test point, where *RPM* = 8,000, the test data agreed better with the simulations by Ye et al.<sup>(54)</sup> and Qing et al.<sup>(63)</sup>, rather than with the original experiments by Grunwald and Goodson<sup>(8)</sup>. In their simulations, Qing et al.<sup>(63)</sup> employed the incompressible RANS equations, in combination with a momentum source method by Rajagopalan and Mathur<sup>(64)</sup> to represent the propeller. Response surface methods and Kriging Surrogate Models were utilised for the optimisation, while the overall *FoM* (Figure of Merit) was chosen as the cost function. The duct inner surface geometry and the propeller chord and twist distributions were set as design variables. The study featured an integrated optimisation of the propeller and the duct, and compared the performance of orthogonal combinations of the base-line/optimised duct/propeller. The integrated optimisation was shown to deliver the best performance in terms of *FoM*. The optimised duct had a larger inlet lip curvature and a higher diffuser angle, resulting in higher suction pressure at the duct lip and higher pressure at the diffuser. The optimised blade had an enlarged tip chord length which was almost comparable to the root chord, while the minimal chord was moved to about 70% span. The twist distribution was changed only slightly. The optimised blade was shown to have the highest induced velocity. The combination of the optimised duct and the base-line propeller caused massive separation on the diffuser surface, right after the rotor disk, and the performance decreased substantially. This was due to an excessive adverse pressure gradient induced by the increased expansion ratio  $\Lambda$ . The optimised propeller, however, brought no flow separation with such large expansion ratio, due to the larger tip chord that injected more momentum into the boundary layer. However, the optimised propeller was not further validated or analysed using blade resolving CFD. Nonetheless, this study puts forward the significance of the integrated optimisation of the overall configuration. A common drawback of studies that adopted actuator disks, is that disk models can hardly account for aerodynamic interactions. Therefore, the

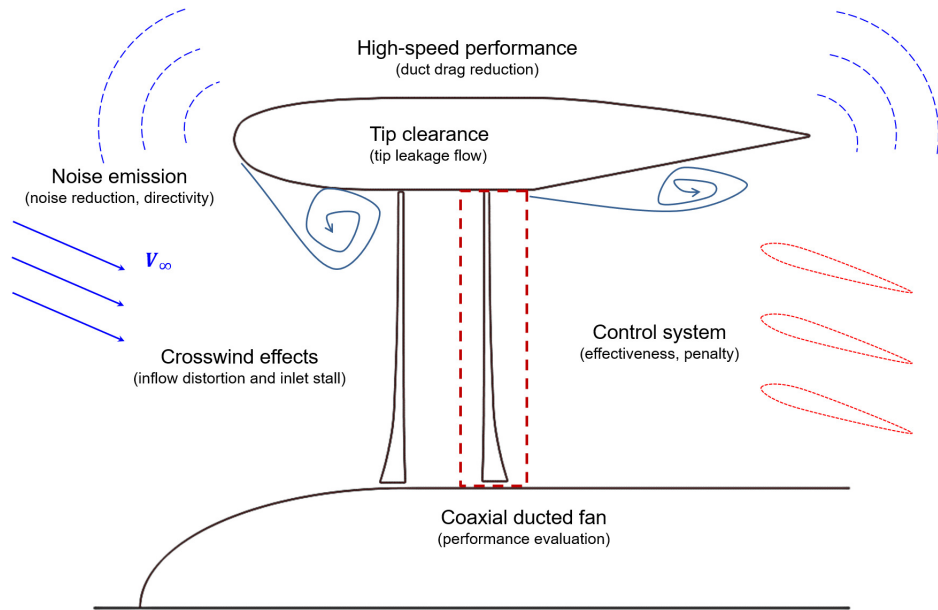


Figure 10. Ducted fan research challenges.

optimisation results, especially for the propeller, may be inaccurate, and need to be further verified.

Optimisation with resolved blade geometries can rarely be found. Biava and Barakos<sup>(57)</sup> applied high-fidelity URANS methods to the analysis and optimisation of a ducted propulsor for Hybrid Air Vehicles (Fig. 3(b)). The simulation first accounted for the realistic shape of the propulsor model, including the radiators and coolers (Fig. 9(h)), then gradient-based optimisation was applied to the blade and the duct, respectively, using a simplified centre-body geometry. Performance comparisons between the ducted and open propeller configurations were made to outline significant aerodynamic benefits brought by the duct, especially in static and low advance ratio cases. However, the simulation pointed out that at high advance ratios, the duct is detrimental to the overall performance due to an excessive drag force. Optimisation of the blade twist and the duct shape moderately increased the overall efficiency (by 2%). The optimised duct shape had a shorter chord length and a larger exit radius. The calculated results agreed well with experimental data on the same model. However, due to the proprietary nature of the propulsor, neither the geometry nor the specific performance data (numerical and experimental) are publicly available.

## 4 DUCTED FAN RESEARCH CHALLENGES

The ducted fan studies discussed so far, focused on various aspects of duct design and performance. It can be summarised that past studies tried to address six research aspects or challenges, as shown in Fig. 10. These challenges are now discussed in detail.

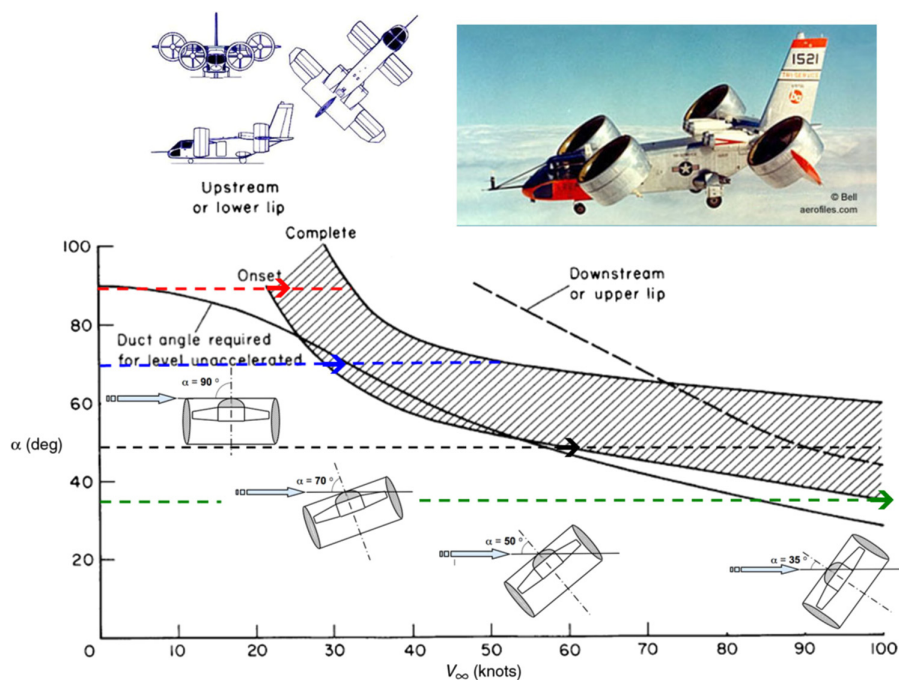


Figure 11. X-22A duct lip stall boundaries.<sup>(20,39)</sup>

#### 4.1 Cross-wind effects

Non-axial inflow results in not only strong aerodynamic forces and moments on the duct, which behaves like an annular wing, but also in imbalanced disk loading that further induces more severe problems such as vibration. Flow separation at the inner or outer duct surfaces may also be encountered. As mentioned earlier, the separation depends on the difference between the fan power and the free-stream speed, the cross-wind angle, and the inlet lip geometry. In fact, several studies<sup>(17,55)</sup> on fan-in-wing types reported lip separation in hover conditions. It is argued that there could be a critical lip radius of 6% duct diameter, below which separation would take place. However, as tested by Graf et al.,<sup>(31)</sup> flow separation was also observed with a radius of 12.5%. Further studies on lip effects were suggested by the researchers.

For tilt-duct aircraft, stall boundaries, as shown in Fig. 11, need to be specified to guide the flight attitude. The cross-wind effects are especially common and severe for ducted fan UAVs, since they tend to fly forward in an edgewise attitude and the Reynolds numbers are relatively low. Similarly, up-stream side flow distortion and separation result in an increase in drag forces and nose-up pitching moments.

Several methods have so far been proposed to alleviate the cross-wind effects, though mostly validated for UAV applications. A double-duct ducted fan concept was proposed by Akturk and Camci<sup>(4)</sup> and Camci and Akturk<sup>(39)</sup>. The idea is to surround the duct with a larger secondary duct. The outer duct is used to adjust the wall static and dynamic pressure allocation, thereby eliminating the inner duct lip separation. Camci and Akturk conducted

CFD simulations using actuator disks, and their effectiveness was compared. However, no comparisons with practical tests can be found.

Myers<sup>(65)</sup> proposed a more straightforward solution by adding vents at the forward flying side of the duct. The vented side almost gives up all benefits brought by the duct, and the asymmetry brings more imbalanced forces. Mechanisms can be introduced to actively open or close the vents according to flight conditions. Grunwald and Goodson<sup>(8)</sup> proposed and examined an increased-radius lip solution that could effectively delay the inner surface separation. His solution resulted in an asymmetric duct since only the upper-stream lip was modified. Similarly, Bahram<sup>(26)</sup> examined asymmetric duct (Fig. 7(k)) configurations, aiming at tilt-duct UAV applications, both experimentally and numerically. Comparing to a symmetric configuration, the asymmetric duct can provide lift forces and smaller force fluctuations during the transition from hover to axial flight. Nonetheless, such a solution may compromise the static performance and bring complexities in the duct geometry.

Actively morphing the duct geometry would be a much better solution for controlling flow separation. Ohanian et al.<sup>(66)</sup> and Kondor and Moore<sup>(67)</sup> applied synthetic jets at the inlet and outlet to insert momentum into the boundary layer, thereby triggering or suppressing flow separation. Further, inlet flow separation can be used to decrease the thrust. Such active flow control technique, that can be seen as a “virtually morphed geometry,” can be an effective way to exert control upon the performance at low speed cases. Its effectiveness on high-speed though needs to be verified. Applying collective and cyclic pitch control to the propeller blades, as implemented by Colman et al.,<sup>(68)</sup> may also be an effective solution, but requires complex mechanisms and will have to be integrated in the small centre body inside the duct. Inlet guide vanes may also be effective in terms of regulating the inflow ahead the rotor disk.<sup>(69)</sup>

Complexity, effectiveness, efficiency, and performance penalties should all be considered to determine the optimal choice. However, whether cross-wind stall remains a severe problem for propulsor applications is arguable. As concluded by Mort<sup>(23)</sup>, the scale of the duct plays an important role in the stall characteristics. For ducted fans that are big enough, e.g. those utilised by the X-22A and the VZ-4, the inlet lip stall can only be encountered at very high rates of descent. Also, in Fig. 11, it can be observed that only mild up-stream inlet stall was encountered during the transition from hover to high-speed flight.

## 4.2 Tip clearance

The clearance between the duct inner surface and the blade tip leads to tip leakage flow. The presence of the duct significantly surpasses the extent of the blade tip vortices and regulates the flow to align with the duct surface, given a small tip-duct clearance. Several experiments, for instance Martin and Tung’s wind tunnel tests<sup>(30)</sup> on a 10-inch-diameter ducted fan, showed that the gap between the blade tip and the duct inner surface, significantly influences the overall thrust and the fan/duct thrust partition. Increasing the tip gap resulted in the thrust dropping quickly. It is also very difficult for wind tunnel experiments to investigate flow features of the tip leakage, due to the geometry of the duct, the very small tip clearance, as well as the blade rotation. CFD simulation represents a better choice in this respect.

Oweis et al. carried out a series of experiments<sup>(70,71)</sup> to study the tip-leakage flow. Although focused on marine applications, their experiments revealed that the size of the primary tip vortex is of the order of the tip clearance, and is not strongly dependent on the Reynolds number, or the boundary-layer thickness. Akturk and Camci<sup>(34)</sup> combined numerical and experimental investigations for a 599mm-diameter ducted fan in hover, and confirmed that a smaller tip gap



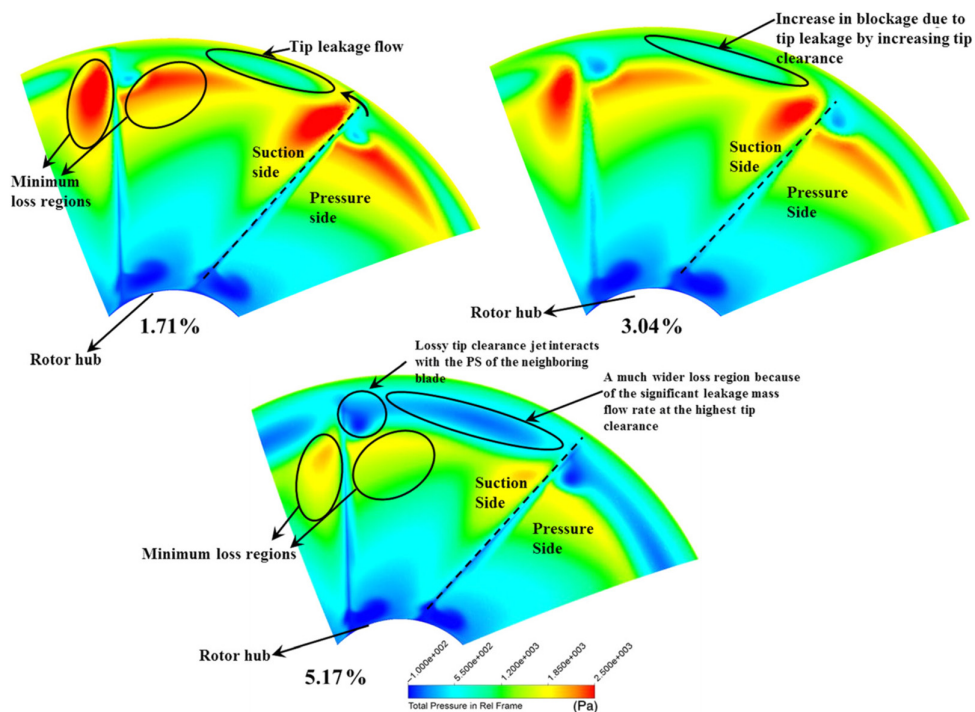


Figure 12. Relative total pressure comparison with different tip clearances.<sup>(34)</sup>

is beneficial. As shown in Fig. 12, through CFD flow-field visualisation, it can be seen that the primary leakage vortices impinged on the neighbouring blade, and the total pressure losses were noticed. As the tip clearance increased, the blade-vortex interaction region grew larger towards the mid-span. They also proposed several blade tip treatments,<sup>(41)</sup> including modifying blade tip shapes and adding tip squealers, to mitigate the performance loss by reducing the leakage vortex strength or changing its trajectory. Matin and Boxwell<sup>(72)</sup> proposed a solution by adding a backward step on the duct inner surface near the rotor disk, but its effectiveness was not strong. More treatments, in terms of blade tip shape and duct shape modifications, or active flow control methods, should be studied and applied to aircraft applications.

Recently, Ryu et al.<sup>(73)</sup> studied the effect of tip clearance for a counter-rotating coaxial ducted fan UAV. Wind tunnel tests were conducted to validate the CFD simulations, while the flow details were studied using CFD. In that study, increasing the front and rear tip clearance caused the  $FoM$  to drop consistently. However, a smaller front rotor tip clearance, in combination with a larger rear tip clearance, delivered the maximum thrust observed. The thrust gain came from the rear rotor. This indicates that in a coaxial configuration, interactions between the two rotors add more complexity, and more detailed analysis is necessary.

### 4.3 High-speed performance

As investigated during many of aforementioned experiments, given the same propeller  $RPM$ , the efficiency of the ducted fan decreases as the advance ratio increases. However, the ratio of the propeller thrust to the overall propulsion increases in the mean time, indicating that the duct's contribution is diminishing fast.

In high speed axial flight, the drag of the shroud may outweigh its benefits if not carefully designed. Early experiments by Krüger<sup>(6)</sup> studied a high speed, high thrust loading ducted propeller model, aimed at reaching 400kg of thrust at 80km/h, and at an altitude of 8.6km, when scaled to full size. The results showed that as the forward advance ratio increases, the propeller thrust coefficient can be maintained with larger blade pitch, but the duct thrust drops quickly and consequently the overall thrust decreases with increasing advance ratio. The experiments also suggested that high speed efficiency can be significantly increased by adopting shroud profiles with smaller chord and thickness, yet this is accompanied by a static performance penalty (that could be mitigated by an outward nose ring). Grunwald and Goodson's experiments<sup>(8)</sup> also found that the propeller to overall thrust ratios increased from 40% to 70% as the forward advance ratio increased from 0 to 0.595 at zero angle-of-attack, indicating a reduction of the duct efficiency at high speed. The experiments of Abrego et al.<sup>(28)</sup> on a 38-inch diameter, fixed-pitch ducted fan, showed that with increasing advancing ratio, the thrust coefficient and efficiency drops quickly.

More recently, Biava and Barakos<sup>(57)</sup> investigated the effect of the duct using high-fidelity CFD methods and concluded that the duct has a significantly positive effect on the overall thrust and efficiency at low speeds. As an extreme, at zero propeller advance ratio the ducted fan could generate 24% more thrust with 25% less power. The visualisation of the flow-field pointed out that the rear part of the duct serves as a diffuser to slow down the wake speed and increase the static pressure, thereby increasing the overall thrust comparing to the free propeller. The efficiency, however, gradually decreases as the advance ratio increases and eventually becomes negative. It is reasonable to conclude that the deficiency is mostly attributed to the greater duct drag caused by the higher speed. Geometric optimisation of the duct rear part was also applied, resulting in a shorter chord length, and a higher expansion ratio, bringing a small performance improvement.

#### 4.4 Noise emission

The ducted fan noise is a separate topic of research. Noise emission of fans enclosed by a duct of finite/infinite/semi-infinite length has attracted great research interest during the past decades. Applications can be found in turbofan/turbomachinery<sup>(74–76)</sup> and environment control device<sup>(77)</sup> noise predictions. A more comprehensive review in this respect can be found in references<sup>(78–81)</sup>.

The ducted fan noise mostly comes from the rotating fan and interactions of its wake with the stator/vane. The presence of the duct substantially modifies the acoustic characteristics of a rotating fan/propeller. Stronger radiation directivity and noise reduction, compared to an open propeller, are the two major features as confirmed by several calculations and experiments. Since the first work by Tyler and Sofrin<sup>(82)</sup> in the 1960s, theoretical/numerical analysis of duct-rotor acoustics has seen significant development. Dunn et al.<sup>(83)</sup> presented a boundary integral equation method for ducted fan noise prediction, and a prediction tool named TBIEM3D<sup>(84)</sup> was developed. The methods were examined by simulating the noise emission of a 20-bladed fan located in the middle of a finite length duct. Twenty(20) spinning point dipole noise sources were placed symmetrically on the fan disk, and the results clearly showed the directivity of the ducted fan noise radiation. In their study, the acoustic pressure was shown to be concentrated around 45° off the rotor rotation axis up-stream and down-stream. The axial and normal directions were left to have minimal sound radiation. The results were compared later by Wang et al.<sup>(85)</sup> using FW-H based methods, and good agreement was noticed. That study complements Hubbard's early experiments.<sup>(15)</sup> Choi et al.<sup>(86)</sup> simulated

the discrete tones of a ducted acoustic source, and also suggested a similar directivity pattern and noise reduction, due to the presence of the duct. Dunn et al.<sup>(83)</sup> also included lined surfaces to evaluate the noise reduction. It was found that inlet and outlet lining is very effective in mitigating the noise radiation.

Most studies mentioned earlier focused on many-bladed, high solidity fans. Though phenomena such as duct reflection and scattering, and rotor/stator interactions, are believed to be similar, fewer analyses can be found for lower solidity ducted fans. Differences in the blade number, *RPM*, pitch angle etc. may result in a shifted characteristic spectrum. As mentioned earlier, Hubbard<sup>(15)</sup> compared sound-pressure measurements of five duct-propeller combinations in hover, with an open propeller at approximately the same rotational speed and power. The geometries of the four ducts, and the two blades tested, along with the test conditions were reported in detail. Total sound pressure, measured 30 feet away, produced by the two-blade shrouded propeller, was constantly lower at all measured angular stations, given no flow separation was present. The maximum measured value was around half that of the open propeller. The measurements also showed clear directivity of the sound radiation. The maximum value was around 70° relative to the rotation axis downstream, while another smaller spike was spotted at about 50° upstream. Lower values were noticed in axial and normal directions to the outer duct surface, with the lowest values along the inflow axis. The results showed that the duct reduced the strength of radiated sound and redistributed the sound energy in different directions. However, when the *RPM* and rotor power were slightly reduced, and flow separation was present at the inner surface near the inlet lip, excessive sound pressure was recorded. The measurements were almost twice as high as the two-bladed open propeller in all directions, and the directivity pattern was maintained. The tests also investigated factors such as the duct chord length, tip clearance, tip speed, and blade number. It was eventually concluded, as also briefly summarised by Bulaga<sup>(87)</sup> later, that many factors which promote the aerodynamic performance also reduce noise emissions, e.g. smaller tip clearance and avoiding flow separation. Reduced *RPM* and increased blade numbers provided better acoustic performance, while the duct chord length had minor effects on the acoustics. The tests, however, were conducted outdoors, hence environmental uncertainties could not be eliminated. Regardless, the study revealed that separation, which was likely to appear at low rotational speeds, leads to higher sound pressure levels. Hubbard's works provided the exact geometry of the ducts and blades (including blade sections). However, limited aerodynamic performance data, which was extracted from the duct surface pressure measurements, was presented.

Recent small-sized experiments reported insignificant or negative noise reduction due to the duct. Martin and Boxwell<sup>(72)</sup> studied the acoustic characteristics of a 10-inch-diameter ducted fan UAV. They concluded that the shroud does not alter the blade passage frequency noise, but increases the level of the broadband noise component. The influence of the tip clearance was reported as insignificant, but the separation at the inlet lip was found to increase the broadband noise contributions. Rhee et al.<sup>(35)</sup> also conducted a series of wind tunnel tests to study the acoustic characteristics of the ducted fan without cross-wind effects. The comparisons showed that the noise level of the ducted fan was slightly higher than for open rotors when producing the same thrust. The directivity feature of the ducted fan noise was also presented, and was shown to be consistent with Hubbard's tests.<sup>(15)</sup> They suggested that a perforated liner installed inside the duct would effectively reduce the noise. Reasons for the opposite conclusions are not certain, but they might be related to the low Reynolds numbers and flow separation.

Very recently, Malgoezar et al.<sup>(88)</sup> conducted acoustics experiments on a 30-cm-diameter ducted propeller with a Clark-Y profile. Variations of acoustic source types

(an omni-directional source and a propeller) and cases at advance ratios were considered. Comparisons were also made between the ducted and the isolated configurations. The duct was shown to have a significant impact on the frequency distribution and directionality, and noise reduction could be noticed for cases with inflow. For static, hover state, however, noise increase was observed for most harmonics, while the frequency distribution resembled more an omni-directional source. Beamforming was then utilised to discern the acoustic sources, and a new noise source is identified at the duct leading edge. It was argued that the resonance of the duct and the interaction between the blade vortices and the duct boundary layer were the reasons behind the noise increase.

Compared to an open propeller, the acoustic performance of the ducted fan can be expected to be superior, as the duct provides a basis for further noise treatments e.g. inlet/exhaust liners. Further experiments and high-fidelity simulations on ducted fan noise should, however, be carried out to explore the acoustic benefits. For future VTOL aircraft, ducted fans show great potential especially on stringent noise limits to be imposed on future rotorcraft.

#### 4.5 Control systems

Effective and efficient control of ducted fan performance is another aspect of this survey. Guide vanes are more commonly deployed to vectorise the propulsor thrust. For UAV applications, several methods, as mentioned earlier, such as active flow control at the inlet and outlet,<sup>(66,67)</sup> cyclic pitch control of the blades,<sup>(68)</sup> inlet spoiler,<sup>(29)</sup> exit rotating cylinder using Magnus effects,<sup>(89,90)</sup> etc. show potential for application. Nonetheless, their actual effectiveness and efficiency on aircraft applications remain unclear.

The inlet vanes are capable of altering the effective blade pitch angle, thereby adjusting the overall thrust distribution. In fact, the inlet guide vanes are also useful for regulating the inflow and alleviating the inflow distortion. Outlet vanes are better for deflecting the flow and generating side forces. Nevertheless, all guide vanes bring blockage and weight. Gilmore and Grahame<sup>(69)</sup> tested inlet and exit guide vanes on a 28.56-inch diameter, fan-in-wing ducted fan model in transitional flight. Ten(10) inlet vanes were allowed to turn individually according to the inflow conditions, while the exit vanes were linked collectively. The experiments showed that the transition performance was improved, by using the inlet vanes for inflow regulation and the exit vanes for aircraft control. As expected, a small performance penalty at static conditions was noticed.

Experiments of the 4-foot ducted fan<sup>(18,24)</sup> also examined both inlet and outlet guide vanes. The experiments concluded that the exit vanes are more effective than the inlet vanes. Abrego et al.<sup>(28)</sup> examined a ducted fan with two 3-inch chord exit vanes, and concluded that exit vanes with flaps are effective in generating side forces. Using a symmetric installation of vanes and deflection angles ( $\pm 40^\circ$ ) the force coefficients were not symmetric, and with zero deflection, slightly positive side-forces were generated. This might be the result of manufacturing defects of the model, as suggested by the authors, but it may also be related to the tangential induction of the rotating rotor. Mort and Gamse<sup>(20)</sup> worked on a full-scale ducted fan with a large vane, and showed symmetric force changes against symmetric deflection angle changes. They also reported that at positive vane deflection angles, the effectiveness of the vane was significantly lower than expected as the cross wind angle was increased. Such asymmetry may also be related to the arrangement of guide vanes. For most tests mentioned herein, the vanes were aligned either in columns or rows, which in itself represents an asymmetry. Other arrangements, such as even distributions along the radius or angular directions, should be considered and evaluated.

Active flow control and cyclic blade pitch control might be possible solutions, as well, but performance penalties should be carefully evaluated. It is to be noted that only few experimental studies considered the effect of the guide vanes, and relevant numerical studies can hardly be found.

#### 4.6 Coaxial ducted fan systems

Adding a second row of rotor blades to the ducted propulsor is important either for emergencies or torque balancing. As mentioned earlier, the contra-rotating coaxial design is also essential to make the ducted fan a compact, removable propulsion unit, which has great potential for future eVTOL aircraft. However, as stated earlier, more complexity in performance analysis should be expected due to the interaction of the two rotors.

Concerning the contra-rotating coaxial ducted fan system, few studies can be found in the open domain and most focused on UAVs, such as the Sikorsky Cypher UAV developed in the late 1990s. Lee<sup>(91)</sup> tested both contra-rotating and single-rotor ducted fan UAV models. He found that, in contrast to the ducted single rotor, shrouding a contra-rotating rotor does not always deliver better performance. Sensitivities to different design parameters, e.g. inlet radius, tip radius, and propeller location, are important. Based on Lee's work, Geldenhuys<sup>(92)</sup> studied a similar coaxial system numerically, using the same duct geometry but used a different rotor design. The DFDC code and incompressible CFD simulations were used for the analysis. The results and experiments matched well, in general, but differences were presented for several cases. It is notable that the DFDC configuration file and elaborate geometric information were provided, making it possible for further validation and investigation. Jiang et al.<sup>(93)</sup> conducted combined numerical and experimental studies on a general coaxial ducted fan configuration. The study mainly investigated three factors: the blade pitch angle, free-stream speed and the rotor spacing. Combinations of these factors gave distinct performance results, yet the CFD results agreed with the experiments very well. Nemnem et al.<sup>(94)</sup> discussed the parameters of coaxial ducted fan design, but the study lacks the support from either experiments or simulations. Overall, performance and determining factors of the coaxial ducted fan need to be further investigated.

## 5 CONCLUSIONS

This survey of published works resulted in the following conclusions:

1. Research on large-scale ducted fans for propulsion purposes mostly emerged between the 1950s and 1970s. Most recent research focused on small-scale UAV applications.
2. Detailed theoretical studies and several lower-order methods for ducted fan performance prediction are available. Higher-order simulations with CFD are within the capability of modern numerical methods and computational resources.
3. Effective treatments for high  $AoA$  distortion/stall, and high-speed performance at high Reynolds number, such as blade tip modifications, asymmetric duct design, deformable geometries, or active flow control methods, need to be investigated.
4. Numerical simulation and multi-objective optimal design of ducted fans should be attempted, and components like stators, second rotors, and guide vanes should be considered.

5. More experiments on ducted fan noise emission should be carried out, and numerical studies should also be explored.
6. Application and performance of ducted fans on compound rotorcraft should be considered and evaluated.

Overall, the ducted fan is a favourable choice as an auxiliary source of lift/thrust for novel rotorcraft configurations considering its benefits, in terms of efficiency, safety, and compactness. However, during the design process, treatments and improvement for cross-wind effects, high-speed performance, noise emission, effective and efficient control system must be investigated and evaluated.

## ACKNOWLEDGEMENTS

The sponsorship of the University of Glasgow and the China Scholarship Council is gratefully acknowledged. The authors are also grateful to the handling editor and the anonymous reviewers for their supportive comments and meticulous reading of the paper.

## References

1. STIPA, L. Experiments with intubed propellers, NACA Technical Memorandum 655, Washington DC, 1932.
2. SACKS, A. and BURNELL, J. Ducted propellers: a critical review of the state of the art, *Prog Aeronaut Sci*, 1962, **3**, pp 85–135.
3. PEREIRA, J.L. Hover and Wind-Tunnel Testing of Shrouded Rotors for Improved Micro Air Vehicle Design, Ph.D. thesis, 2008.
4. AKTURK, A. and CAMCI, C. Double Ducted Fan (DDF) as a novel ducted fan inlet lip separation control device, The International Powered Lift Conference, October 2010, pp 148–170.
5. FLETCHER, H.S. Experimental investigation of lift, drag, and pitching moment of five annular airfoils, Tech Rep, NACA-TN-4117, 1957.
6. KRÜGER, W. On wind tunnel tests and computations concerning the problem of shrouded propellers, Tech Rep, National Advisory Committee for Aeronautics, 1949.
7. PLATT, R.J. Static tests of a shrouded and an unshrouded propeller, Tech Rep, National Advisory Committee for Aeronautics, 1948.
8. GRUNWALD, K.J. and GOODSON, K.W. Aerodynamic loads on an isolated shrouded-propeller configuration for angles of attack from –10 degrees to 110 degrees, Tech Rep, National Aeronautics and Space Administration Washington DC, 1962.
9. CARLTON, J. *Marine Propellers and Propulsion*, 4<sup>th</sup> ed, London, Butterworth-Heinemann, 2018.
10. GILBERT, B., OMAN, R. and FOREMAN, K. Fluid dynamics of diffuser-augmented wind turbines, *J. Energy*, 1978, **2**, (6), pp 368–374.
11. OHYA, Y., KARASUDANI, T., SAKURAI, A., ABE, K.-i. and INOUE, M. Development of a shrouded wind turbine with a flanged diffuser, *J Wind Eng Ind Aerodyn*, 2008, **96**, (5), pp 524–539.
12. GAFFEY, T.M., ZHANG, C., QUACKENBUSH, T.R., SHENG, C. and HASBUN, M. Aeromechanics of the coaxial compound helicopter, 56th AIAA/ASCE/AHS/ASC Structures, Structural Dynamics, and Materials Conference, 2015.
13. JOHNSON, W., ELMORE, J., KEEN, E., GALLAHER, A. and NUNEZ, G. Coaxial compound helicopter for confined urban operations, 2016, pp 210–239.
14. GOODSON, K.W. and GRUNWALD, K.J. Aerodynamic characteristics of a powered semispan tilting-shrouded-propeller VTOL model in hovering and transition flight, Tech Rep, NASA TN D-981, 1962.
15. HUBBARD, H.H. Sound measurements for five shrouded propellers at static conditions, Tech Rep, National Advisory Committee for Aeronautics, 1950.



16. PARLETT, L.P. Aerodynamic characteristics of a small-scale shrouded propeller at angles of attack from 0 to 90 degrees, Tech Rep, NACA-TN-3547, 1955.
17. TAYLOR, R.T. Experimental investigation of the effects of some shroud design variables on the static thrust characteristics of a small-scale shrouded propeller submerged in a wing, Tech Rep, National Advisory Committee for Aeronautics, 1958.
18. YAGGY, P.F. and MORT, K.W. A wind-tunnel investigation of a 4-foot-diameter ducted fan mounted on the tip of a semispan wing, Tech Rep, NASA-TN-D-776, 1961.
19. GRUNWALD, K.J. and GOODSON, K.W. Division of aerodynamic loads on a semispan tilting-ducted-propeller model in hovering and transition flight, Tech Rep, NASA TN D-1257, 1962.
20. MORT, K.W. and GAMSE, B. A wind-tunnel investigation of a 7-foot-diameter ducted propeller, Tech Rep, NASA-TN-D-4142, 1967.
21. BLACK, D. and ROHRBACH, C. Shrouded propellers-a comprehensive performance study, 5th Annual Meeting and Technical Display, 1968, p 994.
22. MORT, K.W. and YAGGY, P.F. Aerodynamic characteristics of a 4-foot-diameter ducted fan mounted on the tip of a semispan wing, Tech Rep, NASA-TN-D-1301, 1962.
23. MORT, K.W. Performance characteristics of a 4-foot-diameter ducted fan at zero angle of attack for several fan blade angles, Tech Rep, NASA-TN-D-3122, 1966.
24. YAGGY, P.F. and GOODSON, K.W. Aerodynamics of tilting ducted-fan configurations, Tech Rep, NASA Langley Research Center, 1961.
25. KRIEBEL, A.R. and MENDENHALL, M.R. Predicted and measured performance of two full-scale ducted propellers, Tech Rep, NASA-CR-578, 1966.
26. BAHRAM, R. Aerodynamic Study of Tilting Asymmetrical Ducted Fans Mounted at the Wing Tips of a VTOL UAV, PhD thesis, 2016.
27. XU, H.-Y., XING, S.-L. and YE, Z.-Y. Numerical study of ducted-fan lip stall suppression based on inflatable leading lip cell, *Procedia Eng*, 2015, **126**, pp 158–162.
28. ABREGO, A.I., BULAGA, R.W. and RUTKOWSKI, M. Performance study of a ducted fan system, The American Helicopter Society Aerodynamics, Acoustics, and Test and Evaluation Technical Specialists Meeting, San Francisco, CA, 2002.
29. FLEMING, J., JONES, T., NG, W., GELHAUSEN, P. and ENNS, D. Improving control system effectiveness for ducted fan VTOL UAVs operating in crosswinds, 2nd AIAA Unmanned Unlimited Conf. and Workshop & Exhibit, 2003, p 6514.
30. MARTIN, P. and TUNG, C. Performance and flowfield measurements on a 10-inch ducted rotor vtol uav, Tech Rep, Army Research Development and Engineering Command, Moffett Field CA, Aviation Aeroflight Dynamics Directorate, 2004.
31. GRAF, W., FLEMING, J. and NG, W. Improving ducted fan UAV aerodynamics in forward flight, 46th AIAA Aerospace Sciences Meeting and Exhibit, 2008, p 430.
32. AKTURK, A., SHAVALIKUL, A. and CAMCI, C. PIV measurements and computational study of a 5-inch ducted fan for V/STOL UAV applications, 47th AIAA Aerospace Sciences Meeting and Exhibit, Orlando, Florida, 2009, p 332.
33. OHANIAN, O., GELHAUSEN, P. and INMAN, D. A compact method for modeling the aerodynamics of ducted fan vehicles, 48th AIAA Aerospace Sciences Meeting Including the New Horizons Forum and Aerospace Exposition, 2010, p 1052.
34. AKTURK, A. and CAMCI, C. Tip clearance investigation of a ducted fan used in VTOL UAVS: part 1: baseline experiments and computational validation, ASME 2011 Turbo Expo: Turbine Technical Conference and Exposition, American Society of Mechanical Engineers, 2011, pp 331–344.
35. RHEE, W., MYERS, L. and McLAUGHLIN, D. Aeroacoustics of vertical lift ducted rotors, 15th AIAA/CEAS Aeroacoustics Conference (30th AIAA Aeroacoustics Conference), 2013, p 3333.
36. YILMAZ, S., ERDEM, D. and KAVSAOGLU, M. Effects of duct shape on a ducted propeller performance, 51st AIAA Aerospace Sciences Meeting including the New Horizons Forum and Aerospace Exposition, 2013, p 803.
37. CHANG, I.-C. and RAJAGOPALAN, R. CFD analysis for ducted fans with validation, 21st AIAA Applied Aerodynamics Conference, 2003, p 4079.
38. LIND, R., NATHMAN, J. and GILCHRIST, I. Ducted rotor performance calculations and comparison with experimental data, 44th AIAA Aerospace Sciences Meeting and Exhibit, 2006, p 1069.
39. CAMCI, C. and AKTURK, A. Double-ducted fan, 2014, US Patent 8,821,123.
40. AKTURK, A. and CAMCI, C. Experimental and computational assessment of a ducted-fan rotor flow model, *J Aircr*, 2012, **49**, (3), pp 885–897.

41. AKTURK, A. and CAMCI, C. Tip clearance investigation of a ducted fan used in VTOL UAVS: part 2: novel treatments via computational design and their experimental verification, ASME 2011 Turbo Expo: Turbine Technical Conference and Exposition, American Society of Mechanical Engineers, 2011, pp 345–357.
42. THWAITES, B. A note on the design of ducted fans, *Aeronaut Q*, 1951, **3**, (3), pp 173–181.
43. THWAITES, B. A note on the performance of ducted fans, *Aeronaut Q*, 1953, **4**, (2), pp 179–185.
44. BONTEMPO, R. and MANNA, M. Solution of the flow over a non-uniform heavily loaded ducted actuator disk, *J Fluid Mech*, 2013, **728**, pp 163–195.
45. BONTEMPO, R. and MANNA, M. Effects of duct cross section camber and thickness on the performance of ducted propulsion systems for aeronautical applications, *Int J Aerosp Eng*, 2016, **2016**, pp 9. doi: [10.1155/2016/8913901](https://doi.org/10.1155/2016/8913901)
46. YOUNGREN, H., DRELA, M. and SANDERS, S. Ducted fan design code, <http://web.mit.edu/drela/Public/web/dfdc/>, December 2005.
47. BI, N., KIMMEL, K. and HAAS, D.J. Performance investigation of ducted aerodynamic propulsors, First International Symposium on Marine Propulsors, Smp, Vol. 9, 2009.
48. KO, A., OHANIAN, O. and GELHAUSEN, P. Ducted fan UAV modeling and simulation in preliminary design, AIAA Modeling and Simulation Technologies Conference and Exhibit, 2007, p 6375.
49. AHN, J. and LEE, K. Performance prediction and design of a ducted fan system, 40th AIAA/ASME/SAE/ASEE Joint Propulsion Conference and Exhibit, p 4196.
50. AHN, J. and DRELA, M. Newton method on axisymmetric transonic flow and linearized 3D flow prediction, 36th AIAA Aerospace Sciences Meeting and Exhibit, 1998, p 928.
51. DRELA, M. and YOUNGRE, H. Axisymmetric analysis and design of ducted rotors, <http://web.mit.edu/drela/Public/web/dfdc/DFDCtheory12-31.pdf>, December 2005.
52. GUERRERO, I., LONDBERG, W.K., GELHAUSEN, P. and MYKLEBUST, A. A powered lift aerodynamic analysis for the design of ducted fan UAVs, 2nd AIAA Unmanned Unlimited Conference and Workshop & Exhibit, 2003, p 6567.
53. RAJAGOPALAN, R. and ZHANG, Z. Performance and flow field of a ducted propeller, 25th Joint Propulsion Conference, 1989, p 2673.
54. YE, K., YE, Z.-Y. and QU, Z. Aerodynamic optimization method for duct design, *J Aerosp Power*, **28**, 08 2013, pp 1828–1835.
55. SHENG, C., ZHAO, Q. and BI, N.P. Numerical investigations of ducted fan hover performance for FIW applications, 53rd AIAA Aerospace Sciences Meeting, 2015, p. 1935.
56. JIMENEZ, B.G. and SINGH, R. Effect of duct-rotor aerodynamic interactions on blade design for hover and axial flight, 53rd AIAA Aerospace Sciences Meeting, 2015, p 1030.
57. BIAVA, M. and BARAKOS, G.N. Optimisation of ducted propellers for hybrid air vehicles using high-fidelity CFD, *Aeronaut J*, 2016, **120**, (1232), pp 1632–1657.
58. CHEN, J., LI, L., HUANG, G. and XIANG, X. Numerical investigations of ducted fan aerodynamic performance with tip-jet, *Aerosp Sci Technol*, 2018, **78**, pp 510–521.
59. RUBIO, R.C., DIAZ, P.V. and YOON, S. High-fidelity computational analysis of ducted and coaxial rotors for urban air mobility, Proceedings of the 75th Annual Forum, Philadelphia, May 2019.
60. SINGH, R., JIMENEZ, B. and AVERA, M. Investigation of aerodynamic interactions in ducted rotor systems, The AHS 70th Annual Forum, 2014.
61. LI, L., HUANG, G., CHEN, J. and YUAN, J. Numerical experiment of tip-jet ducted fans with various nozzles, 53rd AIAA/SAE/ASEE Joint Propulsion Conference, 2017, p 5093.
62. SCHALLER, D.F. A Technique for Shape Optimization of Ducted Fans, Master's thesis, Iowa State University, 2007.
63. QING, J., HU, Y., WANG, Y., LIU, Z., FU, X. and LIU, W. Kriging assisted integrated rotor-duct optimization for ducted fan in Hover, AIAA Scitech 2019 Forum, 2019, p 0007.
64. RAJAGOPALAN, R.G. and MATHUR, S.R. Three dimensional analysis of a rotor in forward flight, *J Am Helicopter Soc*, 1993, **38**, (3), pp 14–25.
65. MYERS, L.M. Aerodynamic Experiments on a Ducted Fan in Hover and Edgewise Flight, Master's thesis, 2009.
66. OHANIAN, O.J., KARNI, E.D., LONDBERG, W.K., GELHAUSEN, P.A. and INMAN, D.J. Ducted-fan force and moment control via steady and synthetic jets, *J Aircr*, 2011, **48**, (2), pp 514–526.

67. KONDOR, S.A. and MOORE, M. Experimental investigation of a morphing nacelle ducted fan (NASA/CP-2005-213509), 2004 NASA/ONR Circulation Control Workshop, 16–17 March 2004, 2004, pp 435–468.
68. COLMAN, M., SUZUKI, S., and KUBO, D. Wind tunnel test results and performance prediction for a ducted fan with collective and cyclic pitch actuation for VTOL with efficient cruise, AIAA Atmospheric Flight Mechanics Conference, 2011, p 6379.
69. GILMORE, A. and GRAHAME, W. Research studies on a ducted fan equipped with turning vanes, *J Am Helicopter Soc*, 1959, **4**, (4), pp 11–21.
70. OWEIS, G.F., FRY, D., CHESNAKAS, C.J., JESSUP, S.D. and CECCIO, S.L. Development of a tip-leakage flow - part 1: the flow over a range of Reynolds numbers, *J Fluids Eng*, 2006, **128**, (4), pp 751–764.
71. OWEIS, G.F., FRY, D., CHESNAKAS, C.J., JESSUP, S.D. and CECCIO, S.L. Development of a tip-leakage flow - part 2: comparison between the ducted and un-ducted rotor, *J Fluids Eng*, 2006, **128**, (4), pp 765–773.
72. MARTIN, P. and BOXWELL, D. Design, analysis and experiments on a 10-inch ducted rotor VTOL UAV, American Helicopter Society (AHS) International Specialists Meeting on Unmanned Rotorcraft: Design, Control and Testing, Chandler, AZ, January, 2005, pp 18–20.
73. RYU, M., CHO, L. and CHO, J. The effect of tip clearance on performance of a counter-rotating ducted fan in a VTOL UAV, *Japan Society*, 2017, **60**, (1), pp 1–9.
74. RUMSEY, C.L., BIEDRON, R., FARASSAT, F. and SPENCE, P. Ducted-fan engine acoustic predictions using a Navier–Stokes code, *J Sound Vib*, 1998, **213**, (4), pp 643–664.
75. NARK, D., FARASSAT, F., POPE, D.S. and VATSA, V. The development of the ducted fan noise propagation and radiation code CDUCT-LARC, 9th AIAA/CEAS Aeroacoustics Conference and Exhibit, 2003, p 3242.
76. REBOUL, G., POLACSEK, C., LEWY, S. and HEIB, S. Aeroacoustic computation of ducted-fan broadband noise using LES data, *J Acoust Soc Am*, 2008, **123**, (5), pp 3539–3539.
77. SHUR, M., STRELETS, M., TRAVIN, A., CHRISTOPHE, J., KUCUKCOSKUN, K., SCHRAM, C.F., SACK, S. and ÅBOM, M. Effect of inlet distortions on ducted fan noise, 22nd AIAA/CEAS Aeroacoustics Conference, 2016, p 2819.
78. EVERSMAN, W. Theoretical models for duct acoustic propagation and radiation, 1991.
79. GROENEWEG, J.F., SOFRIN, T., RICE, E. and P.R., G. *Aeroacoustics of Flight Vehicles: Theory and Practice, Vol 1: Turbomachinery noise*, chap. 3, NASA Rep 1258, 1991, pp. 151–210.
80. MOTSINGER, R. and KRAFT, R. Design and performance of duct acoustic treatment, In: *Aeroacoustics of Flight Vehicles: Theory and Practice*, Vol. 2, Chap. 14, NASA Rep 1258, 1991, pp. 165–206.
81. ASTLEY, R., SUGIMOTO, R., ACHUNCHE, I., KEWIN, M., MUSTAFI, P. and DEANE, E. A review of CAA for fan duct propagation and radiation, with application to liner optimisation, *Procedia Engineering*, Vol. 6, 2010, pp 143–152.
82. TYLER, J.M. and SOFRIN, T.G. Axial flow compressor noise studies, Tech Rep, SAE Technical Paper, 1962.
83. DUNN, M., TWEED, J. and FARASSAT, F. The application of a boundary integral equation method to the prediction of ducted fan engine noise, *J Sound Vib*, 1999, **227**, (5), pp 1019–1048.
84. DUNN, M.H. TBIEM3D: a computer program for predicting ducted fan engine noise. Version 1.1, Tech Rep, NASA/CR-97-206232, 1997.
85. WANG, T., YANG, B. and GUAN, Y. A study on the prediction of the ducted fan noise, 11th AIAA/CEAS Aeroacoustics Conference, 2005, p 3069.
86. CHOI, H.L., JEON, W. and LEE, D.-J. Duct effects on aeroacoustic noise of an axial fan, ICA 2004, Acoustical Society of Japan, 2004, pp 3261–3264.
87. BULAGA, R. Ducted fan efficiency and noise, Aerospace Technology Conference and Exposition, 2005.
88. MALGOEZAR, A.M., VIEIRA, A., SNELLEN, M., SIMONS, D.G. and VELDHUIS, L.L. Experimental characterization of noise radiation from a ducted propeller of an unmanned aerial vehicle, *Int J Aeroacoust*, 2019.
89. ZHAO, J., HOU, Q., JIN, H., ZHU, Y. and LI, G. CFD analysis of ducted-fan UAV based on magnus effect, 2012 IEEE International Conference on Mechatronics and Automation, IEEE, 2012, pp 1722–1726.

90. HOU, Q.-M., ZHU, Y.-H., ZHAO, J., LI, G. and JIN, H.-Z. A novel ducted-fan UAV model using magnus effect steering engine, *J Aeronaut Astronaut Aviat*, 2014, **46**, (3), pp 209–217.
91. LEE, T.E. Design and Performance of a Ducted Coaxial Rotor in Hover and Forward Flight, Master's thesis, University of Maryland.
92. GELDENHUYS, H.J. Aerodynamic Development of a Contra-Rotating Shrouded Rotor System for a UAV, Master's thesis, Stellenbosch University.
93. JIANG, Y., LI, H. and JIA, H. Aerodynamics optimization of a ducted coaxial rotor in forward flight using orthogonal test design, *Shock and Vibration*, 2018, **2018**, pp 9. doi: [10.1155/2018/2670439](https://doi.org/10.1155/2018/2670439)
94. NEMNEM, A.F., ZAKARIA, M.Y. and ELZAHABY, A.M. Contra-rotating ducted fan aerothermodynamic design procedure for unmanned applications, 2018 AIAA Information Systems-AIAA Infotech@Aerospace, 2018, p 0745.